Chapter 3

Silicate & Carbonate Weathering in the Himalaya: Impact on major ion chemistry and $^{87}Sr/^{86}Sr$ of the Ganga Headwaters

The impact of silicate and carbonate weathering in regulating the major ion composition and $^{87}Sr/^{86}Sr$ of the headwaters of the Ganga-Ghaghara-Indus is discussed in this chapter. This has been achieved by (i) making new measurements on the chemical composition and $^{87}Sr/^{86}Sr$ of the extensive Precambrian carbonate deposits from the Lesser Himalaya and in a few headwaters of the Ganga-Ghaghara-Alaknanda system (Singh *et al.*, 1998) and (ii) analysing available data on the chemical and Sr isotope composition of these rivers (Sarin *et al.*, 1989; Krishnaswami *et al.*, 1992; Sarin *et al.*, 1992; Pande *et al.*, 1994 and Trivedi *et al.*, 1995) and granite/gneisses/metasediments from the Lesser and Higher Himalaya (Kashyap 1972; Misra *et al.*, 1973; LeFort, 1975; Rao, 1983; Bhattacharya *et al.*, 1984; Rawat 1984; Nautiyal and Rawat, 1990; Choudhury *et al.*, 1991; Gupta *et al.*, 1994; Kaur and Chamyal, 1996)

It is well established that the $^{87}Sr/^{86}Sr$ of the oceans has been steadily increasing through the Cenozoic (Veizer, 1989; Richter *et al.*, 1992). The sources contributing to this increase has been a topic of considerable interest and debate. It has been attributed to recent mountain building activities, e.g. the Himalaya, and associated enhanced chemical weathering of silicates (Raymo and Rudimann, 1992). This will have effect on global climate change as enhanced silicate weathering would cause drawdown of CO_2 from the atmosphere contributing to cooling. Subsequently, Palmer and Edmond (1992) suggested that the high $^{87}Sr/^{86}Sr$ in the Himalayan rivers is due to the weathering of metamorphosed carbonates which have acquired high $^{87}Sr/^{86}Sr$ from the mobilisation of radiogenic Sr from silicates during metamorphism. This inference was based on the observation that the major ion chemistry of the Ganga is dominated by carbonate weathering and the mixing line between $^{87}Sr/^{86}Sr$ and (1/Sr) of the river waters predicted a value of 0.7209 for the high Sr endmenber generally taken to be carbonates. If carbonates are indeed the source for the high $^{87}Sr/^{86}Sr$ in the headwaters, then under steady state it would not affect CO_2 balance of the atmosphere. Thus it is important to understand the source(s) of the high $^{87}Sr/^{86}Sr$ in these rivers, which will provide better insight into the coupling between tectonics, chemical weathering and global change. In this context, a major emphasis of this thesis has been to assess the role of silicate and carbonate weathering in contributing to the major ion chemistry and Sr isotope composition of rivers draining the southern slopes of the Higher and Lesser Himalaya. Data on the chemical and isotopic

composition of granite/gneissess of the region are available in literature, whereas there is almost no data on carbonates. Therefore, a detailed investigation of the large carbonate outcrops of the Lesser Himalaya through which the headwaters of the major rivers flow was undertaken.

The Precambrian carbonate deposits, occurring in abundance all across the Lesser Himalaya, in the drainage basins of the several of the headwaters of Ganga-Ghaghara-Indus, were collected from different locations (Fig. 3.1) and were analysed for their mineralogy, chemical composition and Sr, C, O isotopes to study their importance in contributing to the present day chemistry and Sr isotope composition of the Himalayan rivers. In addition, the studies of the composition of ancient sedimentary carbonates provide a means to constrain the chemical and isotopic evolution of the seawater through time. The measured isotopic and chemical composition of ancient carbonates is a result of their original composition (i.e., at the time of their deposition) and postdepositional overprinting on their original signatures. Veizer (1983), Hall and Veizer (1996) have used covariation trends in the elemental and stable isotope systematics to identify and to select "least altered" carbonates for paleoceanographic research. Some of these approaches have been followed to obtain *qualitative* information on the alteration effects in the samples analysed. Main goal of this study, however, is to assess the importance of these carbonate deposits in contributing to major ions and Sr isotopes to the river waters which currently flow through them.

3.1. MINERALOGY, CHEMICAL AND ISOTOPIC COMPOSITION OF THE PRECAMBRIAN CARBONATES

(i) Mineralogy and Chemical Composition

Thin section microscopy and XRD studies helped in the identification of various minerals present in the Precambrian carbonates analysed in this study. Chemical composition measurements also provided an idea of their mineralogical composition of the carbonates. The mineralogical and chemical composition of the samples analysed are given in Table 3.1. Microscopic studies reveal that most of the samples are micrites, some are made of spars and microspars. Polycrystalline rhombs of calcite are scattered within the micrite/micro-sparite groundmass. The grain margins are often blurred due to

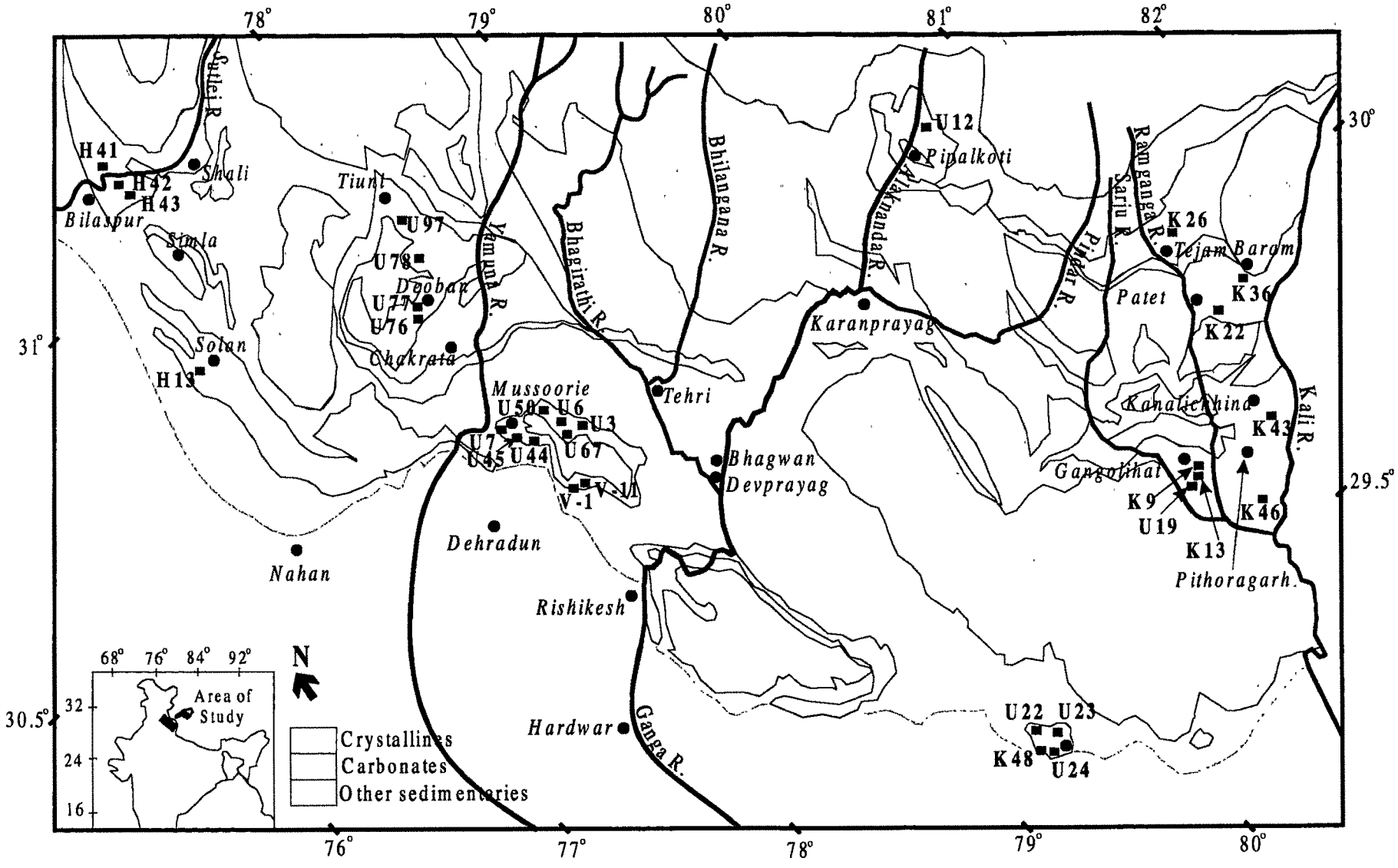

Fig. 3.1: Precambrian carbonate exposures in the Lesser Himalaya and the sampling locations. The sample numbers are abbreviated, e.g., K9 corresponds to KU92-9, U97 is UK94-97.

Table 3.1 : Chemical & mineralogical composition of carbonate rocks from the Lesser Himalaya

Code*	Formation	Location	Ca (%)	Mg (%)	Al (%)	Mn ppm	Rb ppm	Sr ppm		Petrography[$]
INNER BELT										
Gangolihat - Pithoragarh										
KU92-9[+]	Mandhali	Dasaithal	16.7	9.1	0.09	2036	1.4	41	D, Q	dolomite with calcareous silt and quartz veins
KU92-13[+]	Deoban	Gangolihat	22.1	12.7	0.03	235	52	66	D, Q	dolomicrite
UK95-19	Deoban	Gangolihat	29.2	1.05	0.05	80	1.5	114	C, Q,D	microspars of calcite and dolmite
KU92-43[+]	Deoban	Kanalichina	12.5	6.9	1.3	1610	45	84	D, Q	dolomicrite with veins of calcite
KU92-46[+]	Mandhali	Pithoragarh	7.2	5.4	4.76	481	165	48	Q, D	dolomitic marly slate
Thal -Tejam - Pipalkoti										
KU92-22[+]	Mandhali	Patet	17.9	10.4	0.14	86	22	30	D, Q	impure dolomitic marble
KU92-26[+]	Deoban	Tejam	20.6	12.2	0.25	121	5.5	22	D, Q	impure dolomitic marble
KU92-36[+]	Mandhali	Baram	16.5	9.3	0.18	413	5.4	68	D, Q	dolomicrite with quartz filled fractures
UK95-12	Mandhali	Pipalkoti	21.5	12.2	0.4	179	8.6	24	D	dolomitic microspar
Shali - Bilaspur										
HP94-41[+]	Shali	Salapar	34.3	0.22	0.48	462	7.9	104	C, Q	micrite with calcite veins
HP94-42[+]	Shali	Salapar	36.1	0.77	0.42	221	14.6	124	C, Q	micrite
HP94-43[+]	Shali	Salapar	21.4	10.1	0.09	114	2	20	D, C	dolomicrite with calcite veins
Chakrata - Deoban - Tiuni										
UK94-76	Deoban	Jari	37.1	0.18	0.37	108	-	325		
UK94-77	Deoban	Jari	21.1	12.0	0.01	62	-	33		
UK94-78	Deoban	Jari	25.8	6.3	2.6	130	-	363		
UK94-97	Deoban	Lokh Khandi	22.5	12.6	0.07	46	-	52		
OUTER BELT										
Dehradun-Mussoorie										
UK94-44[+]	Krol	Dehradun	36.4	1.0	0.05	17	0.05	282	C, D	micrite with dolomite
UK94-45[+]	Krol	Dehradun	39.6	0.25	0.01	11	0.05	305	C	micrite with calcite veins
UK94-50	Krol	Mussoorie	34.8	3.3	0.01	75	0.17	173	C, D	spary calcite with dolomite
UK95-3	Krol	Mussoorie	36.1	3.5	0.01	54	0.5	147	C, D	micrite with spary dolomite
KU92-55[+]	Krol	Maldeota	19.0	10.9	0.86	351	23	141	D,Q	dolomicrite
UK94-67	Krol	Suakholi	22.6	13.1	0.06	141	-	52	D, C	dolomite with calcite veins

UK95-6	Krol	Barlowganj	22.7	12.8	0.01	77	0.24	33	D	dolomite spar
UK95-7	Krol	Kempty-Fall	20.5	11.9	0.2	102	8.2	240	D	dolomicrite with spars filled fractures
VKC-11	Krol	Mussoorie	22.9	9.3	0.27	1370	4.9	62		
VBL-1	Blaini	Mussoorie	21.7	11.3	0.23	1840	1.8	53		
Nainital										
KU92-48[+]	Krol	Nainital	21.4	12.3	0.09	1190	1.7	95	D	dolomicrite
UK95-22	Krol	Nainital	22.7	12.4	0.02	533	0.18	52	D	clayey dolomite
UK95-23	Krol	Nainital	22.4	11.8	0.08	1667	0.18	67	D	microspars of dolomite with dolomite veins
UK95-24	Krol	Nainital	23.0	11.9	0.05	1533	0.15	44	D	dolomite
Solan										
HP94-13[+]	Krol	Solan	25.6	11.0	0.03	175	-	-	D, C	dolomite with calcite
SPITI VALLEY										
SPT-5(Gypsum)		Spiti	24.4	-	0.03	46	0.4	1027		

* KU - Kumaun, HP - Himachal Pradesh, UK - Uttarakhand, the two digits following the alphabets represent the year of collection.
The VBL-1, VKC-11 and SPT-5 (Spiti) samples provided by Dr. K. K. Sharma

$ based on X-ray and thin section studies, D: Dolomite, Q : Quartz, C: Calcite from XRD
Ca, Mg, Al and Mn abundances in the whole rock samples, * measured by AAS, others by ICP-AES. Rb and Sr by TIMS except in UK94-76, 77, 78 and UK94-97 where Sr by ICP-AES.

recrystallisation. The micrite ground mass are often cut with veins filled with secondary calcite or quartz (Fig. 3.2). Secondary silica growth and opaque hexagonal grain are also seen in some of the samples (Fig. 3.3). In many samples, pore spaces or veins are filled with cements whereas in some of them original carbonate fragments are distributed in cements deposited later. In some of the samples, particularly those collected close to the MCT, effects of metamorphism is seen from the presence of schistosity (Fig. 3.4). During mountain building process, near the MCT, due to high temperature and pressure part of the carbonates could have been converted to marble. The thin section studies, thus show evidence for alteration of these carbonates.

X-Ray diffraction studies show pronounced peaks of dolomite and calcite in most of the samples (Fig. 3.5) whereas in a few of them quartz peaks are also present. Microscopic and XRD studies and chemical composition measurements all suggest that many of these carbonates are predominantly made of dolomite, the few exceptions being the limestones from Shali-Bilaspur in the inner belt and Dehradun-Mussoorie in the outer belt (Table 3.1).

The average **bulk** chemical composition of dolomites and limestones from the inner and outer belts are given in Table 3.1 and their average in Table 3.3. Most of the samples contain abundant Mg, consistent with that expected based on X-ray diffraction studies. Among the samples analysed only five of them had Mg $\leq$ ~1% (UK95-19, HP94-41, HP94-42, UK94-76, UK94-44 and UK94-45) others had Mg 3.3-12.8% (Table 3.1) with Mg/Ca (molar) 0.008 to 1.25. The Al content of carbonate rocks were generally low, except in three samples from the inner belt where it was in excess of 1% (KU92-43, KU92-46 and UK94-78). The high Al content in the inner belt samples is due to their association with shale/slate (rhythmites). Often they are intercalated with layers of varying thickness of shales or slates. The low Al, particularly in the outer belt samples, suggests that these carbonate rocks are generally pure with very low aluminosilicate contamination. The concentration of Rb showed considerable variation, 0.05-165 ppm, the highest concentration was in sample KU92-46 which also had the highest Al (Table 3.1). Statistical analysis of Rb and Al data show a strong positive correlation between them (correlation coefficient 0.94) indicating a common source for both, aluminosilicates. A covariance plot of Mn with Al doesn't show any discernible trend

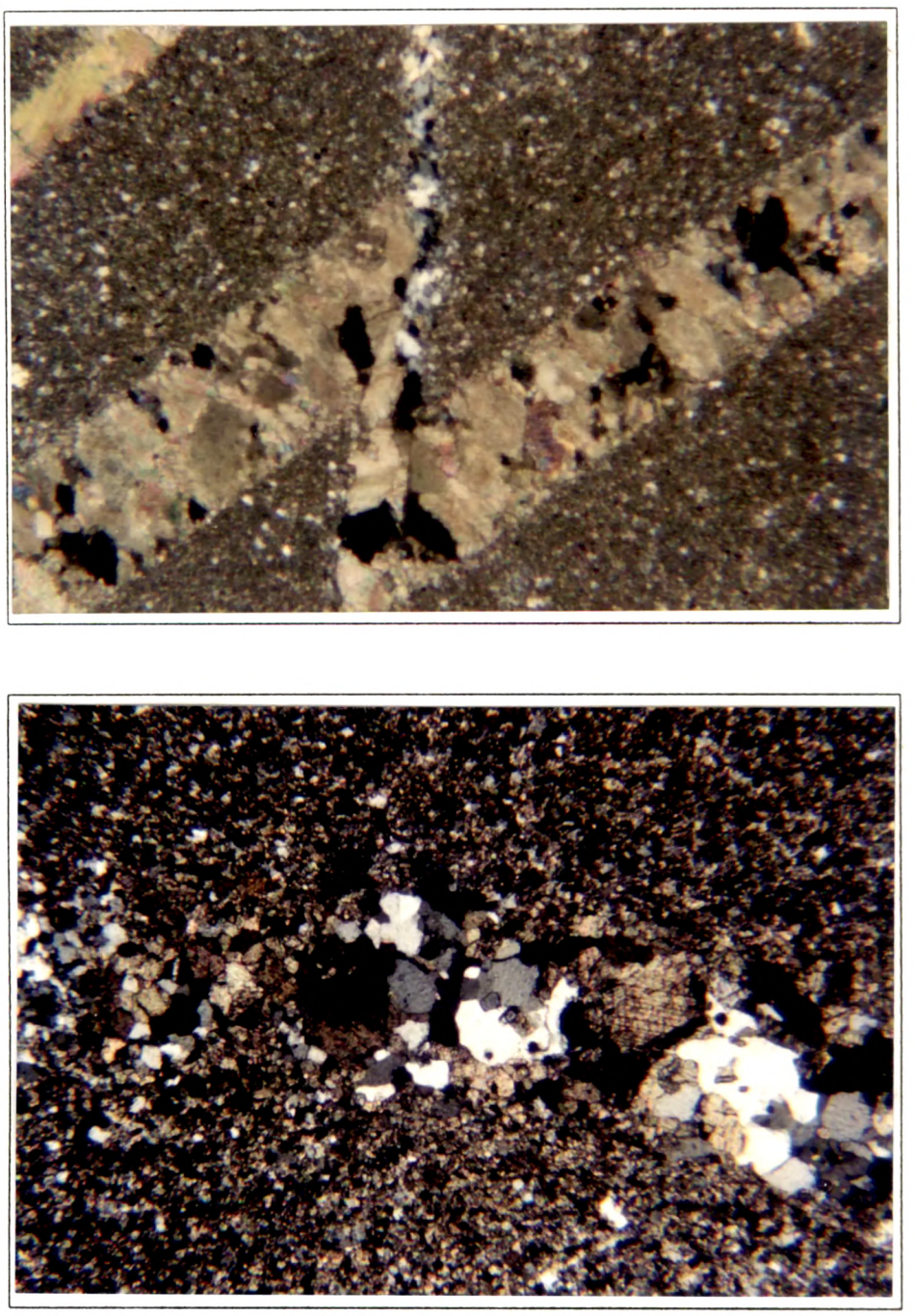

a

b

Fig. 3.2: Thin section photographs. (a) Sample # KU92-36; Micrite groundmass is cut with spar filled veins. Some of the veins are filled with quartz.; Mgnification 25X, Cross Nicols. (b) Sample # KU93-43; Vein filling in microspar. Vein consists dominantly of quartz and large calcite grains. Quartz show recrystallisation texture. Magnification 25X, Cross Nicols.

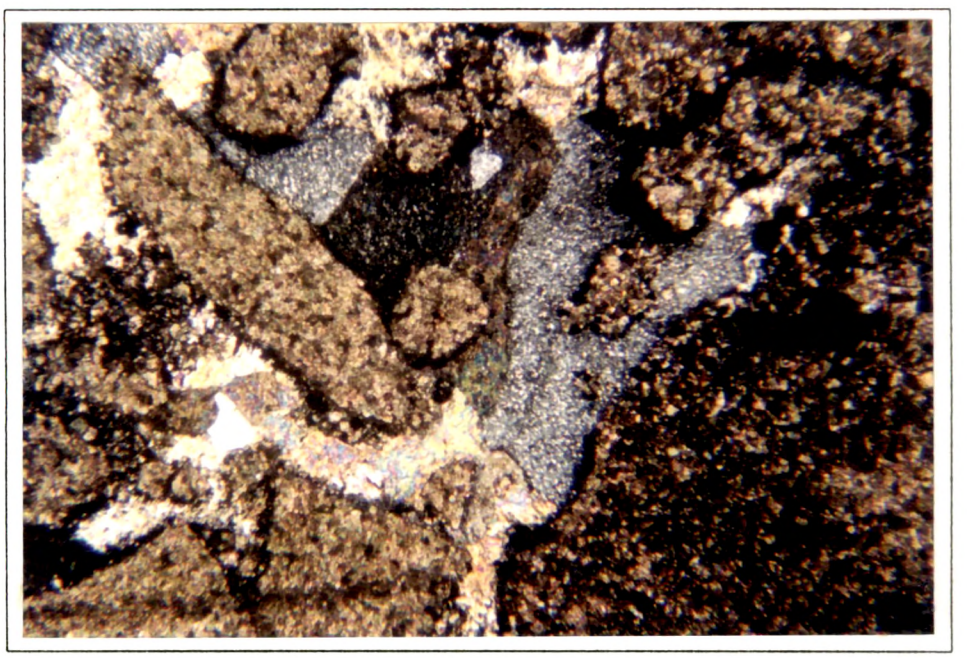

Fig. 3.3: Sample # HP94-13. Bracciation in microspar. Fractures are filled with secondary silica and calcite cements. Magnification 25X; Cross Nicols.

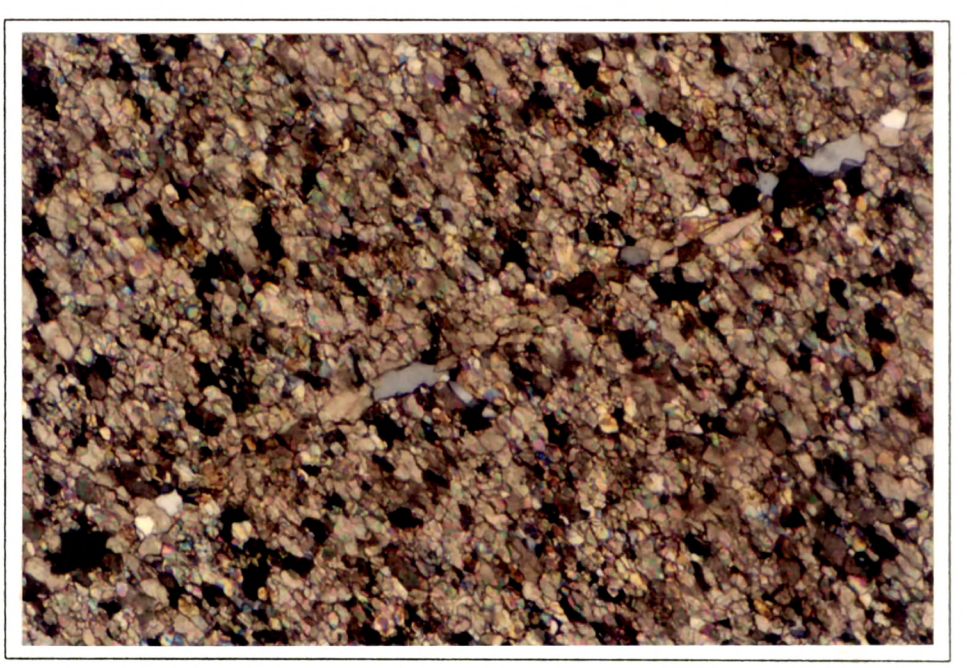

Fig. 3.4: Sample # KU92-26 was collected from near MCT. Grains are euhedral equant and alongated. Schistosity has developed due to pressure. Quartz rich veins following the schistosity plane as well as cross-cutting are suggestive of later neomorphism giving a pseudo-marble. Magnification 40X, Cross Nicols.

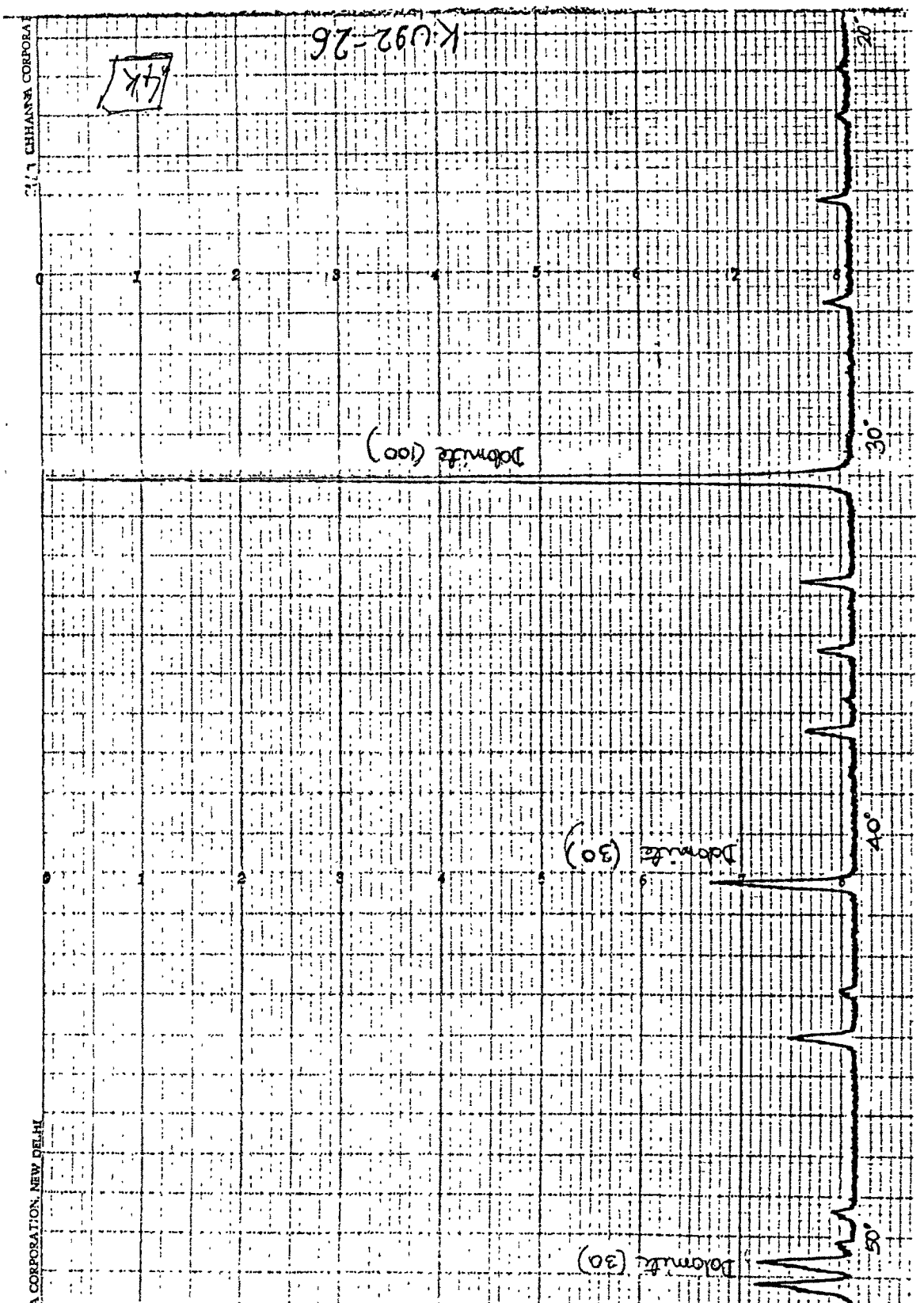

Fig. 3.5: X-Ray diffraction spectrum for sample # KU92-26

which indicates that Mn has been added to the carbonates during their alterations. Broadly, among the dolomites, the samples from the inner belt have higher Al, Rb and $^{87}Sr/^{86}Sr$ (Table 3.3). The high Al in the inner belt samples is consistent with field observations that many of them occur as intercalations of carbonates and shales/slates with significant spatial variability in their relative thicknesses.

The chemistry of the bulk samples (Table 3.1) and their mild acid leaches (0.1N HCl or 5% Acetic acid) show that most (>90%) of the Ca, Mg, Sr and Mn are leachable

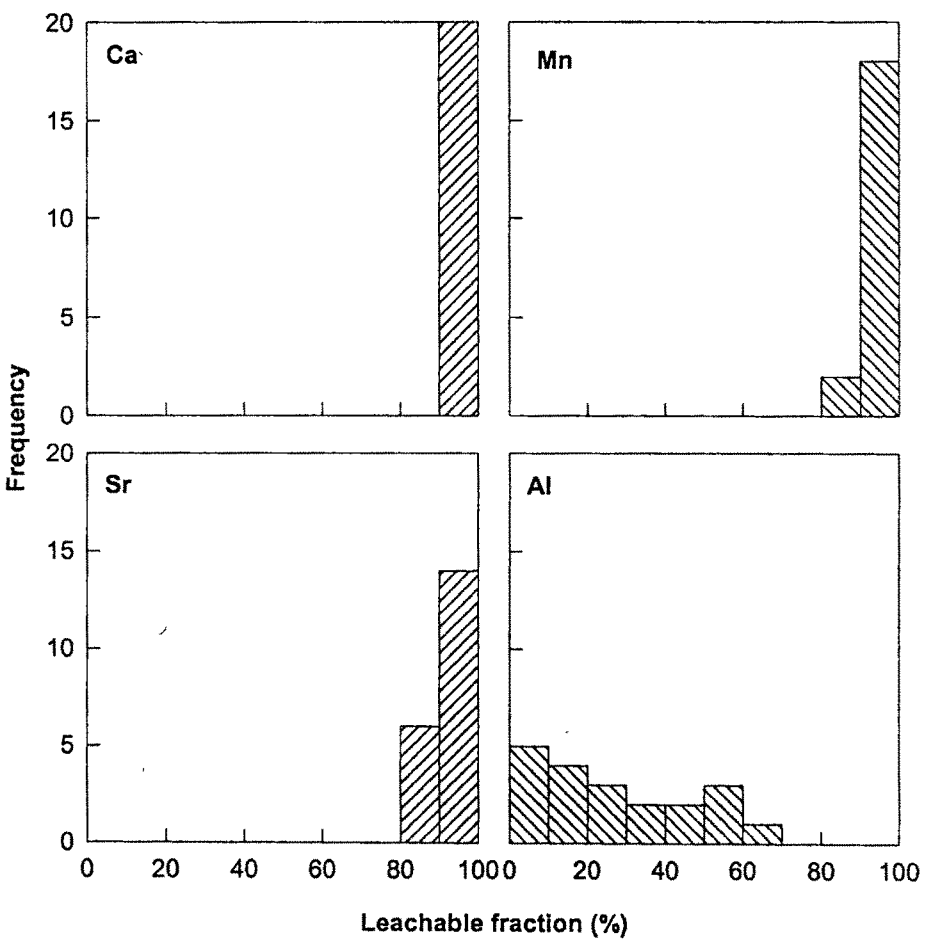

Fig. 3.6: Histogram of leachable fractions of Ca, Mn, Sr and Al in mild acid. Figures show that most of the Ca, Sr and Mn is leachable and hence are associated with the carbonate phase. Leachable Al shows considerable range, probably due to its association with more resistant alumino-silicates

from the bulk rock suggesting that these elements reside almost entirely in the carbonate phase (Fig. 3.6). In contrast, the fraction of leachable Al shows a wide scatter (3% to 64%), averaging ~30%. Among the elements in the carbonate fraction, the abundances of

Sr and Mn are determined by the extent of alteration of the samples (Veizer 1983, Hall and Veizer 1996). During alteration, the carbonate matrix loses Sr and gains Mn and their

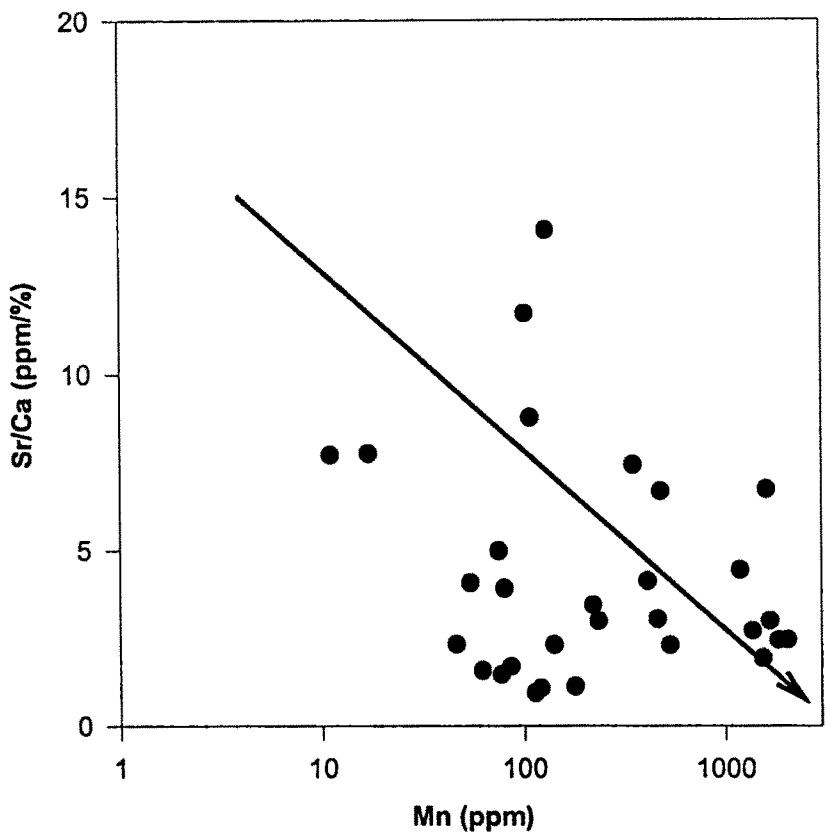

Fig. 3.7: Scatter diagram of Sr/Cs vs Mn in the carbonates analysed. The abundances in the bulk samples are plotted as most of the Sr and Mn are associated with carbonate phase. The overall negative trend is indicative of gain of Mn and loss of Sr suggestive of alteration of the samples.

covariation trend provides a measure of the preservation of their original signatures. The mean concentration of Sr in the dolomites and the limestones from the inner belt are 48 and 148 ppm respectively, in the outer belt samples these are about a factor of two higher (Table 3.3). In general, the concentration of Sr in the carbonates from the Lesser Himalaya are significantly lower than those in recent marine carbonates but are similar to those of Precambrian carbonates (Mirota and Veizer, 1994).

Figure 3.7 is a scatter diagram of (Sr/Ca) vs Mn in the samples analysed, the bulk composition has been plotted as most of the Sr and Mn are contained in the carbonate phase. The data in Fig. 3.7 show an overall negative trend. A possible cause for the

scatter in Fig. 3.7 may be the extent and nature of their alteration and the properties of the endmembers involved. Further in Fig. 3.7 the data of all the samples analysed have been pooled which include limestone and dolomites that are derived from different carbonate formations, Krol, Deoban, Mandhali and Shali which were deposited at different time periods.

(ii) Oxygen and Carbon isotopes

The mean $\delta^{18}O_{(PDB)}$ and $\delta^{13}C_{(PDB)}$ data for the dolomites and limestones from the inner and outer belts overlap with each other, with mean values of ~ -9‰ and ~1‰ respectively (Table 3.3). The $\delta^{18}O$ data show a wide range, -1.4 ‰ to - 12.8 ‰ (Table 3.2) similar to those reported for the Krol carbonates (Bhattacharya *et al.*, 1996 ; Sarkar *et al.*, 1996; Kumar, 1998) and for the Precambrian carbonates from other geographical regions (Veizer and Hoefs, 1976; Hall and Veizer, 1996). The $\delta^{13}C$ values, in comparison show a narrow range, -1‰ to +3.3‰ (Table 3.2), as the carbon isotope pool is dominated by the carbonates. It is known (Mirota and Veizer, 1994) that oxygen isotopes shift towards lighter $\delta^{18}O$ values during dolomitization. Development of fractures and

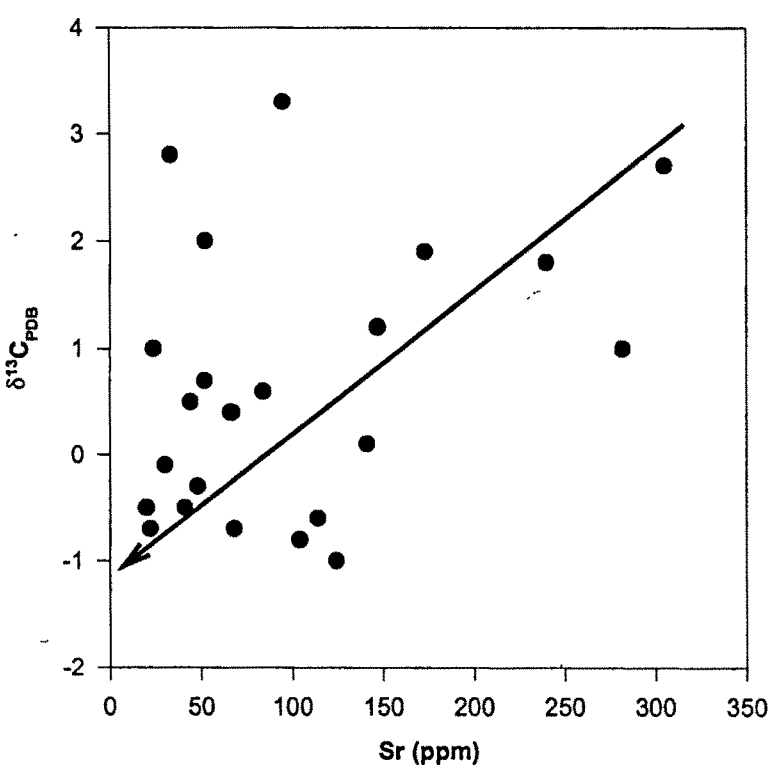

Fig. 3.8: Covariation plot of $\delta^{13}C$ vs Sr. The overall positive trend observed may result from alteration of the carbonates by fresh water causing depletion in $\delta^{13}C$ and removal of Sr.

microfractures due to compaction and/or tectonic activity can provide passage for fluids and pore space that can be filled with cements. Cementation associated with influx of extraneous water commonly leads to alteration of isotopic composition. In fact in many of the samples thin section studies show evidence for cementation. Fig. 3.8 is a plot of $\delta^{13}C$ –vs- Sr, which shows an overall positive trend. The factor(s) contributing to the trend is unclear, a possible explanation could be the alteration of carbonates by fresh water (containing biogenic CO_2) causing depletion in $\delta^{13}C$ and removal of Sr. The quantitative significance of this hypothesis, however, needs to be assessed. Analysis of $\delta^{18}O$ –vs- Mn and $\delta^{18}O$ –vs- Sr data in the carbonates from the Lesser Himalaya, however, did not show any significant covariation.

The present studies based on thin sections microscopy, $\delta^{13}C$, $\delta^{18}O$, Mn, Sr and $^{87}Sr/^{86}Sr$ on the Precambrian carbonates from the Lesser Himalaya all seem to suggest that many of these carbonates have been altered. Attempts were **not** made to study the extent of alteration in greater detail, as it is **not** directly relevant to the main goal of this study, which is to evaluate the role of weathering of these carbonates in contributing to the **present day** major ion and Sr isotope budget of the rivers draining through them. Such a study only requires the knowledge of the chemical and isotopic composition of the carbonates being **currently** weathered and not the details of how their composition has evolved.

(iii) Sr isotope systematics

The Sr isotopic composition of the bulk carbonate rocks and their mild acid leaches show considerable variation, from 0.7064 to 0.8935 (Table 3.2). Most of the samples, however, have $^{87}Sr/^{86}Sr$ in the range of 0.7064 - 0.7300, with two samples from the Gangolihat - Pithoragarh region having extremely high values, 0.8535 and 0.8935 respectively (Table 3.2). The $^{87}Sr/^{86}Sr$ of the leaches are similar to those of the bulk samples (Table 3.2) consistent with that expected as most of the Sr in the bulk rock is leachable (Fig. 3.6). While this work was in progress, Sarkar *et al.* (1996) reported $^{87}Sr/^{86}Sr$ in the carbonate fraction of a few samples from Krol-Tal formations, their $^{87}Sr/^{86}Sr$ numbers, 0.7098-0.7292, bracket our data (Table 3.2). Besides this, data for $^{87}Sr/^{86}Sr$ in carbonates from the Lesser Himalaya are sparse; Galy (1999) reports value of 0.7395-0.8572 with low Sr and Quade *et al.* (1997) values of ~0.73 for detrital carbonates from Nepal rivers. Among

the samples analysed, those from the inner belt have higher $^{87}Sr/^{86}Sr$ ratios. The samples having the most radiogenic ratios are KU92-43 and 46 (Table 3.2) also have high Al content (Table 3.1). Both these samples are rythmites made of layers of carbonates and silicates. The Sr isotope ratio of the carbonate fraction of these samples also are highly radiogenic with values in excess of 0.85 (Table 3.2). Two other bulk samples which have $^{87}Sr/^{86}Sr$ in excess of 0.73 are KU92-26 and 36 (Table 3.2). KU92-26 is from the northern Thal-Tejam region an area which is reported to be affected by enhanced metamorphism (Bhattacharya, 1982) and KU92-36 was collected at the contact with gneiss. The Sr isotope composition of mild acid leaches of these samples are also quite radiogenic, attesting to the influence of alteration processes in the redistribution of Sr isotopes between silicates and carbonates. These results lead us to infer that the Sr isotope systematics of many carbonates from this region have been modified by postdepositional addition of radiogenic Sr.

The chronology of the carbonates analysed in this study is not well established. However, based on stromatolites Valdiya (1980) has inferred that the Deoban, Mandhali, Shali were deposited during Middle Riphean to Vendian and the Krol during Late Precambrian. The $^{87}Sr/^{86}Sr$ during this period was 0.705-0.707 (Veizer, 1989). The $^{87}Sr/^{86}Sr$ of the carbonate fraction of many samples analysed in this study are significantly higher than that of seawater of that time, 0.705-0.707 (Veizer, 1989) suggesting postdepositional addition of radiogenic Sr to the carbonates. Widespread metamorphism and magmatism in the Himalaya involving large-scale fluid transport could have caused loss of Sr from the carbonate and redistribution of Sr isotopes between coexisting silicates and carbonates resulting in the formation of carbonates with low Sr content and high $^{87}Sr/^{86}Sr$. Sr isotope composition can also be modified near the carbonate-silicate boundary by diffusive processes. During metamorphism fluids containing Sr can diffuse into the carbonates and silicates and modify their isotopic signatures (Bickle *et al.*, 1995; Gazis *et al.*, 1998).

Table 3.2 : Sr,O & C isotopic data on carbonate rocks from the Lesser Himalaya

Code	Sr ppm	Whole Rock $^{87}Sr/^{86}Sr$	Leach $^{87}Sr/^{86}Sr$	$\delta^{13}C$(PDB)* (‰)	$\delta^{18}O$(PDB)* (‰)
INNER BELT					
Gangolihat - Pithoragarh					
KU92-9	41	0.7102	-	-0.5	-11.5
KU92-13	66	0.7064	-	0.4	-9.1
UK95-19	114	0.7067	-	-0.6	-9.0
UK95-19(R)		0.7068			
KU92-43	84	0.8786	0.8935	0.6	-12.5
KU92-46	48	0.8901	0.8535	-0.3	-9.1
Thal -Tejam - Pipalkoti					
KU92-22	30	0.7147	-	-0.1	-10.2
KU92-26	22	0.7323	0.7314	-0.7	-6.4
KU92-36	68	0.7314	0.7173	-0.7	-10.9
UK95-12	24	0.7286	0.7246	1.0	-9.0
Shali - Bilaspur					
HP94-41	104	0.7219	0.7219	-0.8	-9.7
HP94-42	124	0.7171	0.7159	-1.0	-11.2
HP94-42(R)	-	-	0.7158		
HP94-43	20	0.7144	0.7138	-0.5	-6.5
Chakrata - Deoban - Tiuni					
UK94-76	325		0.7087		
UK94-77	33		0.7162		
UK94-78	363		0.7102		
UK94-97	52		0.7081		
OUTER BELT					
Dehradun-Mussoorie					
UK94-44	282	0.7093	0.7089	1.0	-12.8
UK94-45	305	0.7124	0.7097	2.7	-9.2
UK94-50	173	0.7098	0.7095	1.9	-12.5
UK95-3	147	0.7102	-	1.2	-11.8
KU92-55	141	0.7142	-	0.1	-8.7
UK94-67	52	-	0.7147	0.7	-9.8
UK95-6	33	0.7093	-	2.8	-3.9
UK95-7	240	0.7096	-	1.8	-1.4
VKC-11	62	0.7128	-		
VBL-1	53	0.7139	-		
Nainital					
KU92-48	95	0.7141	0.7148	3.3	-3.6
UK95-22	52	0.7088	-	2.0	-9.7
UK95-23	67	0.7108	-	0.4	-10.3
UK95-24	44	0.7107	-	0.5	-12.1
Solan					
HP94-13	-	-	0.7109	1.7	-7.6
SPITI VALLEY					
SPT-5(Gypsum)	1028	0.7082	-		

(R) - repeat measurement
* no fractionation correction was made for dolomites

Table 3.3 : Mean composition of carbonate rocks from the Lesser Himalaya

	Inner Belt				Outer Belt				All samples	
	Dolomite		Limestone*		Dolomite		Limestone*			
Element	mean+	log1σ	mean+	log1σ	mean+	log1σ	mean+	log1σ	mean	σ
Ca (%)	18.0	0.15	34.0	0.05	23.8	0.08	38.0	0.03	24.3	7 7
Mg (%)	9 6	0.13	0.42	0 38	9.6	0.20	0.50	0.43	8 3	4 7
Al (%)	0.32	0.94	0.21	0.46	0.06	0.67	0 02	0.49	0.43	0 95
Sr (ppm)	48	0.34	148	0.23	83	0.28	293	0 02	109	98
Mn (ppm)	219	0.52	172	0.34	349	0.59	14	0.13	501	635
Rb (ppm)	12	0.69	6	0.51	0.89	0.78	0.05	-	15	34
Isotopes	mean	1σ	mean	1σ	mean	1σ	mean	1σ	mean	1σ
$\delta^{13}C$ (‰)	-0.1	0.6	-0.8	0.2	1.5	1.0	1.9	1.2	0 7	1 2
$\delta^{18}O$ (‰)	-9.5	2.1	-10.0	1.1	-8.3	3.8	-11.0	2.6	-9.1	2 9
$^{87}Sr/^{86}Sr$	0 745	0.066	0.714	0.007	0.712	0.002	0.711	0.002	0.725	0.043

+ geometric mean, all other arithmatic mean, data from Tables 3.1 and 3.2

* Carbonates having ≤ ~1% Mg is considered as limestones. Samples UK95-19, HP94-41 & 42 and UK94-76 of the inner belt, UK94-44 & 45 of the outer belt fall in this category.

Table 3.4: Range in Sr abundance and $^{87}Sr/^{86}Sr$ in carbonates from the Lesser Himalaya

Sample/location	Sr (ppm)	$^{87}Sr/^{86}Sr$	Ref.
Lesser Himalaya Pc. Carbonates	20-363	0.7064-0.8901	**This work**+
Detrital Carbonates Nepal, Siwalik	NA	0.722 - 0.734	Quade *et al*, 1997
Lesser Himalaya	28-55	0.7395-0.8572	Galy, 1999
Krol Belt	252-588	0.70976-0.72918	Sarkar *et al.*, 1996

+ : Whole rock data (Table 3.2)

NA: Not Available

(iv) Impact of carbonate weathering on $^{87}Sr/^{86}Sr$ of the Ganga-Ghaghara-Indus Headwaters

One of the unique characteristics of the G-G-I source waters is their high $^{87}Sr/^{86}Sr$ and Sr concentration (Palmer and Edmond, 1989; Edmond, 1992; Krishnaswami *et al.*, 1992;Palmer and Edmond, 1992; Pande *et al.*, 1994; Trivedi *et al.*, 1995). The source(s) for the high $^{87}Sr/^{86}Sr$ is still debated and includes weathering of granites/gneisses (Krishnaswami *et al.*, 1992; Edmond, 1992), metasediments (Harris, 1995) and metamorphosed carbonates (Palmer and Edmond, 1992). Quade *et al.* (1997) based on $^{87}Sr/^{86}Sr$ studies of soil carbonates from the Siwaliks and detrital carbonates from the rivers of Nepal have suggested that carbonates are important and perhaps dominant source for the high $^{87}Sr/^{86}Sr$ in the rivers of the Himalaya. Harris *et al.* (1998) and Blum *et al.* (1998) based on the analysis of Bhote Kosi and Raikhot rivers, two minor tributaries of the Ganga and Indus respectively, for their major ion chemistry and Sr isotopes also have highlighted the importance of carbonate weathering in contributing to the Sr flux and high $^{87}Sr/^{86}Sr$ of the Himalayan rivers. The suggestion of Palmer and Edmond (1992) stems from the observation that the major ion chemistry of G-B rivers is dominated by carbonate weathering and that the covariation trend between $^{87}Sr/^{86}Sr$ and (1/Sr) predicts a value of 0.7209 for the high Sr end member, generally taken to be carbonates. Interestingly the mean $^{87}Sr/^{86}Sr$ of the bulk carbonates analysed in this study, 0.725 (Table 3.3) is very similar to that estimated by Palmer and Edmond (1992). Our results on carbonates show that their $^{87}Sr/^{86}Sr$ are generally <0.72, though a few samples have values as high as ~0.85 (Table 3.2; Fig. 3.9). The river water $^{87}Sr/^{86}Sr$ are always in excess of 0.72 (Krishnaswami *et al.*, 1992, Pande *et al.*, 1994, Trivedi *et al.*, 1995; Fig. 3.9). Therefore, if carbonates have to be an important source for the high $^{87}Sr/^{86}Sr$ of the headwaters, then carbonates with adequate Sr and high $^{87}Sr/^{86}Sr$ (comparable to those in headwaters) have to be exposed over wide areas of the Himalaya. Both these conditions are not met by the Precambrian carbonate outcrops of the Lesser Himalaya, the largest carbonate exposure in the drainage basins of many of these headwaters. These carbonates have low Sr and $^{87}Sr/^{86}Sr$ generally <0.720. These observations lead to the conclusion that the weathering of these Precambrian carbonates **cannot be** a major source for the high radiogenic Sr to these rivers on a basinwide scale, though they can be important for

some tributaries which flow through carbonates with extraordinarily radiogenic Sr isotope composition. A more detailed discussion on the source(s) of radiogenic Sr to the headwaters is presented in the next section.

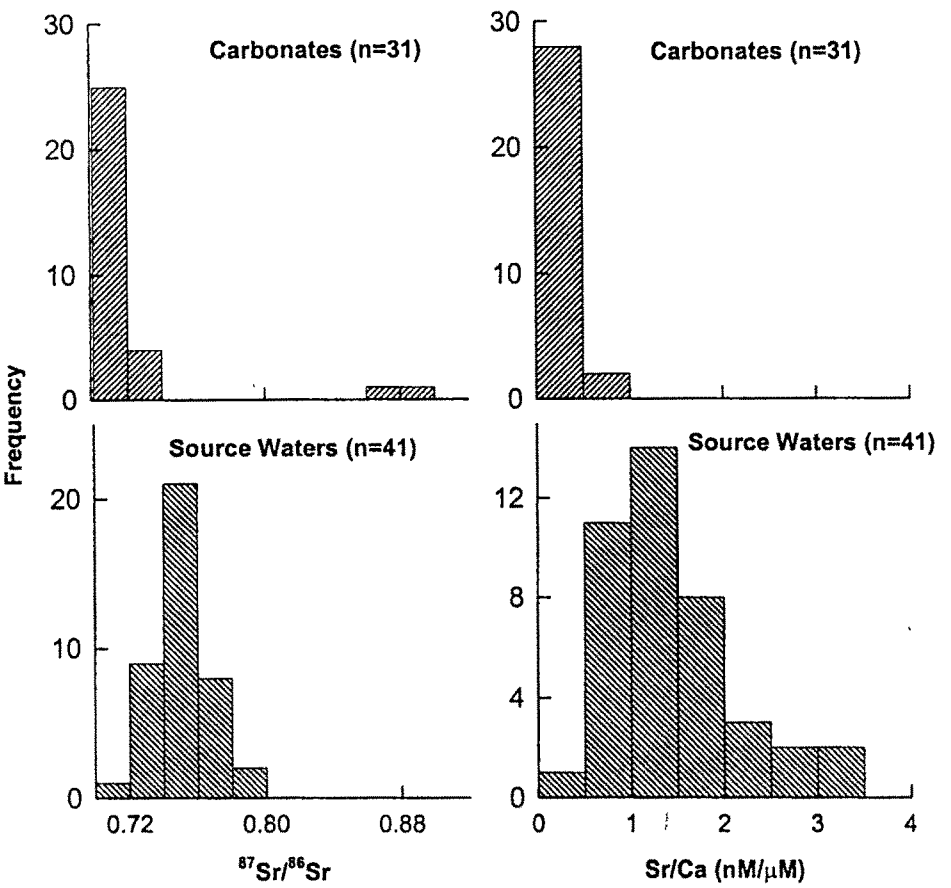

Fig.3.9: Histograms showing the comparison $^{87}Sr/^{86}Sr$ and Sr/Ca in the G-G-I source waters and Precambrian carbonates. Both $^{87}Sr/^{86}Sr$ and Sr/Ca in the headwaters are much higher than those of the Precambrian carbonates.

(v) Sr contribution from Precambrian carbonates to the headwaters

An upper limit on the carbonate Sr to the headwaters can be derived by assuming that (i) *all* Ca in the rivers is of carbonate origin and (ii) the Sr/Ca ratio in the carbonates is 0.20±0.15 (nM/μM), the mean value measured in the Precambrian carbonate outcrop (this study; Table 3.3; Fig. 3.9) and (iii) Ca and Sr in these carbonates are getting weathered congruently. The results (Fig. 3.10) show that the carbonate Sr can account for 6 to 44% (mean 18%) of measured riverine Sr. The limit would increase to 11 to 77%, (mean 31%) if the Sr/Ca ratio in the carbonates is taken as 0.35; one sigma over the mean

value. Considering that Ca can also be supplied to these rivers from the weathering of silicates, evaporites, and phosphates the Precambrian carbonate component of Sr in the Himalayan rivers is likely to be lower than that estimated above. These estimates indicate

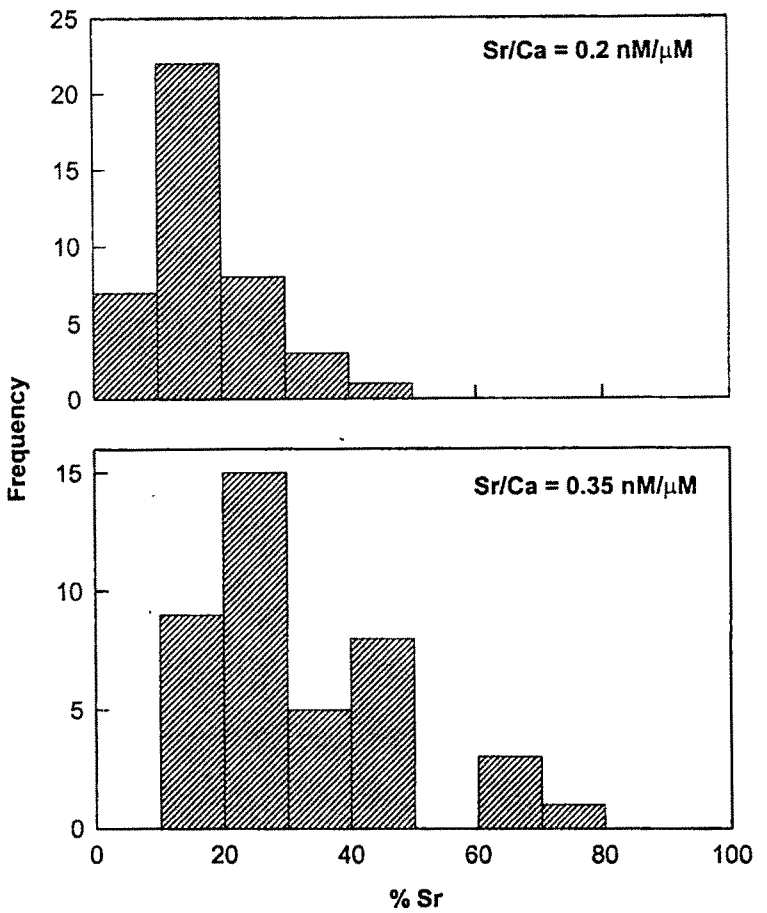

Fig. 3.10: Carbonate Sr component in the G-G-I source waters. The values are *upper limits* and are calculated by assuming that *all* the Ca in the headwaters is of carbonate origin and Sr/Ca in carbonates as 0.2 nM/μM, their mean abundance ratio in Precambrian carbonate outcrops (top) and 0.35 nM/μM, 1σ over the mean abundance ratio in carbonates (bottom).

that bulk of the Sr in most of these rivers has to originate from sources other than Precambrian carbonates of the Lesser Himalaya such as weathering of silicates, evaporites, and phosphates and other carbonates.

The role of carbonates in contributing to the high strontium isotope composition of the source waters is governed by their $^{87}Sr/^{86}Sr$ and their supply of Sr to the rivers. Thus, rivers draining carbonates with $^{87}Sr/^{86}Sr$ of ~0.85, such as those from Gangolihat-

Pithoragarh would have $^{87}Sr/^{86}Sr$ in excess of 0.74, even if the fraction of carbonate Sr in them is only ~18%, the balance Sr being supplied from silicates with $^{87}Sr/^{86}Sr$ of 0.720.

Sarkar *et al.* (1996) and Quade *et al.* (1997) have recently proposed that carbonates are important and perhaps dominant source of high $^{87}Sr/^{86}Sr$ in the rivers of the Himalaya. Sarkar *et al.* (1996) arrived at this conclusion based on the analysis of Krol - Tal carbonates from the Garhwal (Kumaun) Himalaya whereas the suggestion of Quade *et al.* (1997) relies on the $^{87}Sr/^{86}Sr$ measurements of soil carbonates from the Siwalik and detrital carbonates from the rivers of Nepal. The Sr isotope data measured by these two groups and in the present study in the various carbonates overlap with each other and show that many of these are quite radiogenic in composition (Table 3.4). This by itself, however, does not make the carbonates to be a dominant source of the high $^{87}Sr/^{86}Sr$ in rivers, as it would also depend on their contribution to the Sr budget of the rivers. Out of eight samples analysed by Sarkar *et al.*, (1996) five have $^{87}Sr/^{86}Sr$ between 0.720 to 0.729 and the average of all the samples is 0.719 which is slightly higher than the vaverage value of 0.711 obtained in this work for the Krol belt (outer belt) samples (Table 3.3). The Sr concentration measured by acid leaching of the samples are 252 to 588 ppm (Sarkar *et al.*, 1996); their Sr/Ca however is not available as Ca data is not reported. The samples analysed by Sarkar *et al.* (1996) are from the same formation (Krol-Tal) in which measurements have been made in this study. If the mean Sr/Ca ratio of the Krol belt samples analysed in this study (0.21±0.14 nM/μM) is typical of Krol-Tal carbonates from all locations, then they are unlikely to be a major source of Sr to the rivers as their Sr/Ca is significantly lower than in rivers. It is seen from above, that data on both Sr isotopic ratio and Sr/Ca in carbonates are needed to make proper assessment of their role in contributing Sr isotope budget of the rivers. The estimate based on Sr/Ca ratios of Precambrian carbonates measured in this study suggest that on the average they account for only one fifth of the Sr in the source waters. Based on above calculations it can be inferred that the Precambrian carbonates are unlikely to be a major source of high $^{87}Sr/^{86}Sr$ to the rivers on a basinwide scale, however, they could be significant for particular streams.

Harris *et al.*, (1998), based on the study of cations and Sr abundances and $^{87}Sr/^{86}Sr$ in dissolved phase, bed load bulk samples and their leachates of the Bhote Kosi

river, a minor tributary of Ganga, in the Nepal Himalaya concluded that Sr isotope compositions of the headwaters is determined by a small contribution (~10%) from highly radiogenic silicates and ~90% from carbonates which can have $^{87}Sr/^{86}Sr$ upto ~0.8. This inference relies on the Sr isotopic composition determined in leachates of bed loads and an assumed value of 10^{-3} for the molar ratio of Sr/(Ca+Mg) in the carbonates. The leachates have values of $^{87}Sr/^{86}Sr$ in range of 0.712 to 0.792, with a mean of ~0.720, typical of those observed from carbonates analysed in this study. The Sr/(Ca+Mg) of 10^{-3} is much higher than those measured for Precambrian carbonates in this work and suggest the need to have measurements of Sr/(Ca+Mg) in the carbonates drained by the Bhote Kosi. In another study, Blum *et al.* (1998) suggested that vein carbonates present in granite/gneisses of the Higher Himalayan Crystalline Series are contributing to about three fourth of the Sr budget of the Raikhot river in the Higher Himalayan watershed. Based on a Ca/Sr vs $^{87}Sr/^{86}Sr$ plot, they infer that the vein calcites to have Ca/Sr molar ratio 5000 and $^{87}Sr/^{86}Sr$ ~0.82. High $^{87}Sr/^{86}Sr$ of the vein calcite is due the migration of radiogenic Sr to the calcite from the silicates during metamorphism. This is an interesting suggestion and its importance in contributing to the Sr isotope budget of the headwaters can be better assessed if more data on the abundance of vein calcites, their Ca/Sr ratios and $^{87}Sr/^{86}Sr$ become available.

In the following, attempts are made to make elemental and Sr isotope budget for the G-G-I headwaters based on contributions from various sources. Towards this, it is necessary to chemically and isotopically characterise the various endmembers and quantify their contribution to the major ions and Sr isotope composition of the source waters of the Ganga-Ghaghara-Indus. These are discussed below.

3.2. SILICATE AND CARBONATE WEATHERING IN THE GANGA-GHAGHARA-INDUS BASIN: CONTRIBUTION TO THE CHEMICAL AND Sr ISOTOPE BUDGETS OF RIVERS.

(i) Major ion chemistry of the G-G-I source waters

Considerable amount of data on the major ion chemistry of the headwaters of the G-G-I system draining the southern slopes of the Himalaya are available (Sarin *et al.*, 1992; Pande *et al.*, 1994; Trivedi *et al.*, 1995; this study). These results have been

summarised in this section and are used to derive information on the role of silicate and carbonate weathering in the drainage basins. The major rivers of the source waters of the Ganga (Bhagirathi, Bhilangna, Alaknanda, Pindar), the Ghaghara (Sarju, Ramganga, Kali) and the Indus (Beas) all originate in the Higher Himalaya, however, a large fraction of their drainage basins and those of their tributaries lie in the Lesser Himalaya (Fig. 3.1). Sutlej, another major tributary of the Indus has its origin in the Tibetan Plateau and flows through Laddakh and Zanskar before it crosses the Higher Himalaya.

Data on the major ion composition of the source waters of the Ganga, Ghaghara and the Indus and their Sr isotope composition (Table 3.5) are compiled from the earlier publications (Sarin *et al.*, 1989; Krishnaswami *et al.*, 1992; Sarin *et al.*, 1992; Pande *et al.*, 1994; Trivedi *et al.*, 1995). In addition, new measurements on a few samples of the Alaknanda, Pindar, Sarju and Kali are included (RW series, Table 3.5), these samples were collected as a part of this work during Sept 1996, towards the end of the monsoon season.

The chemical composition of rivers at any given site is governed by contributions from the following:

(i) supply of solutes from upstream of the site,

(ii) weathering of local bed rocks and detritus transported to the site from upstream and

(iii) contributions from various tributaries.

Thus, the major ion composition of the Bhagirathi at Devprayag (Fig.3.1), for example, will depend on the input of solutes by weathering all through its drainage basin, from its source in the Gangotri glacier in the Higher Himalaya to Devprayag in the Lesser Himalaya and the supply from its tributaries. Analogous to Bhagirathi, the water chemistry of many major rivers of the Ganga-Ghaghara source waters (e.g. Bhilangna, Alaknanda, Pindar, Kali, Sarju, and Ramganga) would be determined by the bed rock lithologies of both the Higher and Lesser Himalaya as they flow through both these terrains. The chemical weathering rates in the Lesser Himalaya, however, is expected to be higher than those in the Higher Himalaya because of higher temperature, rainfall and the availability of more soil CO_2 for weathering. The material being weathered may involve bed rocks and soils from the Lesser Himalaya and detritus transported from the

Himalayan Crystallines. It is established that significant part of sediments depositing in the Bay of Bengal Fan is transported from the Higher Himalaya (France-Lanord *et al.*, 1993).

Table 3.5: Major ion and Sr concentrations and $^{87}Sr/^{86}Sr$ in G-G-I source waters.

Code	River	Date	Na	K	Ca	Mg	Sr	$^{87}Sr/^{86}Sr$
Ganga								
13	Bhagirathi^{+}	April, 89	141	64	291	103	331	0.7667
16	Bhagirathi	April, 89	131	47	392	170	694	0.7482
10	Bhagirathi	April, 89	145	48	367	139	524	0.7614
11	Bhagirathi	April, 89	193	51	348	144	503	0.7604
8	Bhagirathi	April, 89	150	52	373	134	502	0.7561
4	Bhagirathi	April, 89	163	53	396	149	560	0.7570
5	Bhagirathi	April, 89	154	51	377	136	420	0.7583
23	Bhagirathi	April, 89	154	51	385	134	529	0.7589
RW-3	Bhagirathi	Sept, 96	65	35	249	89		
14	Kedarganga	April, 89	98	83	373	93	262	0.7420
15	Son gad	April, 89	55	56	367	52	315	0.7300
17	Helgu gad	April, 89	51	29	135	31	168	0.7659
9	Pilang gad	April, 89	68	34	179	52	181	0.7902
12	Asiganga	April, 89	42	51	229	60	184	0.7624
7	Nagun gad	April, 89	249	29	555	190	1390	0.7574
6	Seansu gad	April, 89	294	28	394	139	1000	0.7572
19	Bhilangna	April, 89	89	46	288	54	224	0.7554
22	Bhilangna	April, 89	107	49	298	67	246	0.7600
3	Bhilangna	April, 89	115	44	310	93	265	0.7656
20	Jola gad	April, 89	184	31	160	82	273	0.7986
21	Nailchami gad	April, 89	132	61	388	187	431	0.7482
18	Balganga	April, 89	119	36	310	108	367	0.7714
28	Alaknanda^{+}	Oct, 90	44	19	175	23	141	0.7569
29	Alaknanda	Oct, 90	70	40	422	185	650	0.7350
24	Alaknanda	April, 89	107	51	429	175	644	0.7385
RW-4	Alaknanda	Sept, 96	47	36	438	135		
RW-5	Alaknanda	Sept, 96	44	35	420	165		
RW-6	Alaknanda	Sept, 96	51	46	564	232		
RW-7	Alaknanda^{+}	Sept, 96	44	18	187	27		
RW-8	Pindar	Sept, 96	46	37	472	202		
2	Ganga	April, 89	143	51	496	242	676	0.7425
RW-1	Ganga	Sept, 96	65	43	355	122		
RW-2	Ganga	Sept, 96	61	37	316	103		
1	Song	April, 89	283	28	842	432	1310	0.7315
Ghaghara								
R-1	Sarju	Sept, 92	77	33	577		263	0.7585
R-6	Sarju	Sept, 92	71	34	551		311	0.7514

R-7	Sarju	Sept, 92	75	33	551		286	0.7553
RW-9	Sarju	Sept, 96	66	31	645	521		
R-2	Ramganga	Sept, 92	126	30	379		296	0.7757
RW-10	Ramganga	Sept, 96	133	29	338	201		
R-3	Ghat gad	Sept, 92	92	34	609		316	0.7508
R-4	Kali	Sept, 92	65	39	551		1320	0.7276
RW-11	Kali	Sept, 96	53	34	585	367		
R-5	Gori	Sept, 92	78	41	456		768	0.7490
R-8	Panar	Sept, 92	325	52	545		1245	0.7408
R-9	Suyal	Sept, 92	190	39	211		413	0.7351
Indus								
IND-1	Sutlej	Aug, 91	84	82	622	193	1962	0.7166
IND-2	Beas^{+}	Aug, 91	48	25	148	39	169	0.7448
IND-20	Beas^{+}	Aug, 91	22	14	61	18	105	0.7225
IND-3	Chandra^{+}	Aug, 91	24	21	353	76	1118	0.7239
IND-4	Bhaga^{+}	Aug, 91	28	19	332	114	718	0.7342
IND-5	Darcha^{+}	Aug, 91	24	20	189	54	255	0.7595

$^{+}$ samples collected from the Higher Himalaya, all the others from the Lesser Himalaya.
RW-series samples collected in 1996 during this study; R-series Ghaghara source waters [Trivedi *et al.*, 1995]; IND from Pande *et al.*, 1994; others from Krishnaswami *et al.*, 1992; Sarin *et al.*, 1992. The major ion concentrations in μM, and Sr in nM.

Rivers receive major cations and anions from different sources such as atmospheric deposition, weathering of silicates, carbonates and evaporites (Table 3.6). The contribution of these sources to the major ion budget can be assessed if the chemical and isotopic properties of these endmembers are known. These are generally constrained from available data on the bedrocks, soil profiles and stream sediments. Mass balance calculations provide a means to evaluate the contribution from various sources to the river water chemistry.

The mass balance equations for the major cations in rivers are:

$$Na_r = Na_a + Na_e + Na_s \quad (1)$$

$$K_r = K_a + K_s \quad (2)$$

$$Ca_r = Ca_a + Ca_e + Ca_s + Ca_c \quad (3)$$

$$Mg_r = Mg_a + Mg_s + Mg_c \quad (4)$$

$$Sr_r = Sr_e + Sr_s + Sr_c \quad (5)$$

where the subscripts *r*, *a*, *e*, *s* and *c* refer to river, atmospheric, evaporite, silicate and carbonate. The concentrations of major ions in rivers are generally expressed in μM and that of Sr in nM.

Table 3.6: Primary sources of major elements and Sr to river waters.

Element	Major Sources
Na	Atmospheric deposition, solution of evaporites, saline and/or alkaline encrustations, silicate (plagioclase) weathering.
K	Atmospheric deposition, silicate (K-feldspar, biotite) weathering.
Mg	Silicate (olivine, pyroxenes) and carbonate (dolomite) weathering.
Ca	Silicate (plagioclase) and carbonate (limestone, dolomite) weathering, solution of gypsum/phosphorites.
Sr	Same as Ca.

Atmospheric deposition can be an important source of several major ions to rivers. Major ions in the atmosphere are derived from marine, terrestrial and anthropogenic sources. The contribution of atmospheric deposition to the major ion budget of rivers would depend on factors such as vegetation cover, industrial activities in the drainage basins and proximity to the seacoast. Atmospheric deposition fluxes to rivers can be determined through the chemical composition of precipitation (rain and snow) in that region. The chemistry of snow and ice from the Chota Shigri Glacier (Higher Himalaya) and rain water from the foot-hills of Kumaun Himalaya show that atmospheric deposition on an average could account for ~15% of Na and K in the Bhagirathi, Alaknanda and their tributaries (Sarin *et al.*, 1992). For the other major ions, Ca, Mg and SO_4, the atmospheric component is much lower, ≤5%, and hence are neglected in the balance calculations. The Na concentrations in the snow and rain water samples approximately equal that of chloride and hence chloride can serve as the index to determine the Na contribution via atmospheric deposition.

Weathering of evaporites from the drainage basin can be of significance to the mass balance of Na and Ca. As halite is very soluble, its presence in the drainage basins provides an easily weatherable source of Na and Cl to the rivers. The halite component of Na in rivers equals the abundance of chloride. Other sources for Na and K to rivers can

be dissolution of salt encrustations, borax and from alkaline and saline soils. These sources can be important for specific streams (e.g. Yamuna in plains; Indus tributaries flowing through salt encrustations, borax etc.) but are not of significance for rivers discussed in the study.

The silicate component of sodium and potassium in rivers, Na_s and K_s, can be calculated based on the above discussions as:

$$Na_s = Na_r - Cl_r \quad (6)$$

$$K_s = 0.85\, K_r \quad (7)$$

where Cl_r is the measured chloride concentration (μM) in the rivers The Na_s contribution to the Na abundance in the various rivers is calculated as

$$fNa_s = \left[\frac{(Na_r - Cl_r)}{(Na_r)}\right] \times 100 \quad (8)$$

$$f(Na_s+K_s) = \left[\frac{(Na_r - Cl_r) + 0.85K_r}{(Na_r + K_r)}\right] \times 100 \quad (9)$$

The silicate Na component, Na_s, ranges between 27% to 94% of total Na (Fig. 3.11). These calculations show that on an average ~77% of Na and K (range 53 to 90%) in these waters is of silicate origin (Fig. 3.11). The Na_s and K_s together account for 6%-36% (molar fraction) of the total cations and represent the *minimum* contribution of cations to these rivers via silicate weathering. This is a minimum, as silicate weathering would also supply Ca and Mg to the rivers.

The calculation of silicate component of Ca and Mg in rivers is a more difficult exercise as they can be supplied to rivers from several sources and requires some simplifying assumptions to assess the various contributions. In the following, three different approaches are described to determine the silicate Ca or Mg in the rivers. All these methods rely on the estimation of Ca or Mg to Na ratio released to solution from silicates during their weathering. Based on this ratio and the Na_s concentration in rivers estimated earlier, Ca_s is calculated as:

$$Ca_s = \left(\frac{Ca}{Na}\right)_{sol} Na_s \quad (10)$$

where $\left(\frac{Ca}{Na}\right)_{sol}$ is the (Ca/Na) ratio (molar) released to rivers during silicate weathering.

The first approach is to assume that weathering is congruent i.e., during weathering Ca (or Mg) and Na are released to the rivers in the same proportion as their abundances in silicates. The Ca/Na abundance ratios in the granites and gneisses of the

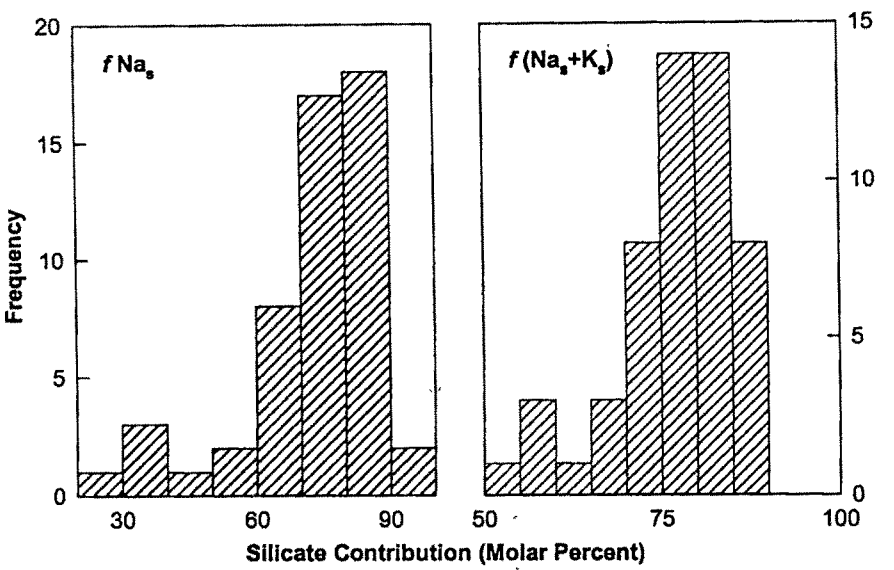

Fig. 3.11: The contribution of Na and Na+K to the G-G-I source waters via silicate weathering. On an average, in the headwaters silicate weathering contributes accounts for ~72% Na and ~77% of (Na+K).

Higher and Lesser Himalaya and in metasediments of the Lesser Himalaya are given in Table 3.7 and their frequency distribution is shown in the Fig. 3.12. The data for the Higher Himalaya are mainly from the Gangotri and the Badrinath regions, the drainage basins of the Bhagirathi, Ramganga, Alaknanda in their upper reaches. The Lesser Himalaya data are mainly from the Kumaun-Garhwal which constitute a major fraction of the drainage basins of the Ganga- Ghaghara source waters. The Ca/Na ratios (μmole/μmole) in the HH and LH samples exhibit a very wide range, spanning nearly three orders of magnitude (Table 3.7, Fig. 3.12). The mean Ca/Na in these fall in the

Table 3.7: Elemental abundance ratios in the HH and LH granites/gneisses and metasediments*

	Granites/Gneisses						Metasediments		
	HH			LH			LH		
	Range	Mean	n	Range	Mean	n	Range	Mean	n
Ca/Na	0.04-1.33	0.27±0.27	58	0.03-7.74	0.68±1.14	78	0.003-2.33	0.39±0.39	77
	0.10-1.33	**0.32±0.29**	**45**	**0.11-1.33**	**0.46±0.28**	**61**	**0.10-1.44**	**0.44±0.31**	**61**
Mg/Na	0.004-10.5	0.40±1.40	56	0.01-20.0	1.51±2.96	78	0.07-8.15	0.77±1.28	77
	0.04-1.31	**0.31±0.28**	**37**	**0.11-2.02**	**0.65±0.45**	**57**	**0.12-1.64**	**0.52±0.32**	**71**
K/Na	0.37-9.02	1.25±1.28	58	0.37-184	6.29±21.3	78	0.13-14.7	2.40±2.36	77
	0.37-3.39	**1.06±0.62**	**56**	**0.37-2.95**	**1.23±0.60**	**63**	**0.47-3.99**	**1.89±1.05**	**60**
Sr/Na	0.17-33.8	1.75±4.44	56	0.08-36.55	2.77±6.69	51			
	0.36-3.0	**1.22±0.65**	**48**	**0.35-3.0**	**1.68±0.72**	**39**			

All ratios in units of μmole/μmole except Sr/Na which is in nmole/μmole. For all ratios two numbers are given. The numbers in bold are the range and the mean obtained by discarding extreme values in the distributions. n: number of samples.

* Sources of data: HH granites/gneisses - [LeFort, 1975; Rao, 1983; Choudhary *et al.*, 1991; Kaur and Chamyal, 1996]; LH granites/gneisses - [Bhattacharya *et al.*, 1984; Rao, 1984; Nautiyal and Rawat, 1990; Gupta *et al.*, 1994;]; LH metasediments - [Kashyap, 1972; Mishra *et al.*, 1973; Rawat, 1984].

range of 0.3 - 0.7 (Table 3.7) with large uncertainties. To obtain a more representative value for the mean Ca/Na with less uncertainties, the Ca/Na data were reanalysed by discarding the extreme values on either end of their distribution (Table 3.7). The recalculated mean Ca/Na and associated errors are given in Table 3.7 which shows that

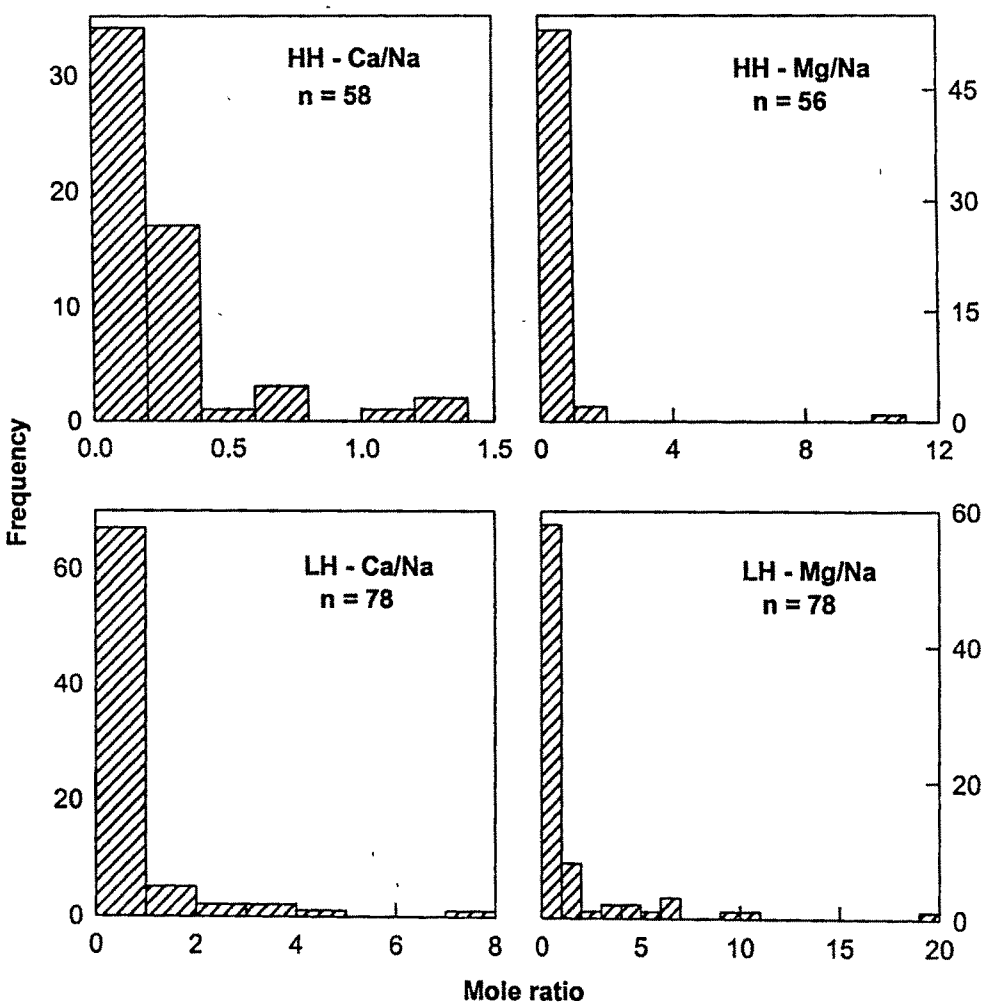

Fig. 3.12: Frequency distribution of Ca/Na and Mg/Na abundances(μmole/μmole) in granites and gneisses of the Higher (HH) and Lesser Himalaya(LH). Data from Le Fort, 1975; Rao, 1983; Bhattacharya *et al.*, 1984; Nautiyal and Rawat, 1990; Choudhury *et al.*, 1991; Gupta *et al.*, 1994; Kaur and Chamyal, 1996.

the mean values in all three groups of samples are nearly the same and centre around a value of 0.45±0.3. The weathering of these silicates, as assumed earlier, would release Na and Ca to rivers in the mole ratio 1 : 0.45.

Another approach to determine the ratio of $(Ca/Na)_{sol}$ is from the measured Ca/Na ratios of streams flowing predominantly through silicate lithology. The Jola gad stream, a tributary of the Bhilangna (Fig. 3.1) meets this requirement. Of all the rivers and streams for which data are available (Table 3.5) Jola gad has the highest $^{87}Sr/^{86}Sr$, lowest Ca/Na and SO_4/HCO_3 (signifying minimum contribution of Ca from carbonates and sulphates). The Ca/Na_s in this sample is 1.15. This value could also be an upper limit of input of (Ca/Na) from silicates as even minor amount of carbonates present in the terrain would add to the Ca in river as they weather far more easily than the silicates.

The third method to estimate the $(Ca/Na)_{sol}$ is from the chemical composition of soil profiles and their parent rocks. Gardner and Walsh (1996) have reported the chemical composition of three soil profiles formed from metamorphic rocks in the Lesser Himalaya. Their results, summarized in Table 3.8, show that Na, Ca and Sr in the soil profiles are significantly less than those in the parent rock, K and Mg in the rocks and soils are quite similar and that Al in the soils is higher than that in the parent rock. These results would indicate that Na, Ca and Sr are mobilised from rocks and soils far more efficiently than Mg and K. The increase in Al (and that of K and Mg in the GW profile) reflects the mass loss during weathering and the resistant nature of Al. From these data, the ratio of various elements to sodium released to rivers during weathering of bed rocks is calculated as:

$$\frac{\left[\left(\frac{X_i}{Al}\right)_{ro} - \left(\frac{X_i}{Al}\right)_{so}\right]}{\left[\left(\frac{Na}{Al}\right)_{ro} - \left(\frac{Na}{Al}\right)_{so}\right]} \qquad (11)$$

where X_i represents the elements Ca, Mg and Sr and the subscripts *ro*, *so* refer to bed rock and soil profile (Table 3.8). The calculations are normalised to Al as it is resistant to weathering and corrects for mass loss. The average value calculated for Ca/Na solution ratio based on the three soil profiles is 0.47 (range 0.37 to 0.52) nearly identical to the mean Ca/Na ratio in the source rocks suggesting that Ca and Na are released to solution by and large in the same proportion as their abundances in the source rocks. The soil profile data provides the element to Na ratio supplied to rivers over the time of soil formation. The three methods employed to determine the $(Ca/Na)_{sol}$ yield values which

Table 3.8: Elemental concentrations and ratios in bed rocks and soil profiles*

Element/Ratio	Bed rock+	Soil Profile++		
		BW1	BW2	GW
Al	2807	3356	3184	3352
Na	644	31	43	135
K	649	622	578	760
Ca	342	19	33	151
Mg	470	425	479	527
Sr	2040	496	699	1114
Na/Al	0.24	0.01	0.01	0.04
Ca/Al	0.12	0.01	0.01	0.05
Mg/Al	0.17	0.13	0.15	0.16
K/Al	0.23	0.19	0.18	0.23
Sr/Al	0.75	0.15	0.22	0.33

* Data from Gardner and Walsh (1996), recalculated in units of μmol/g for all elements except Sr, which is in nmol/g.
+ Average of five samples.
++ BW1 average of 11 samples upto a depth of 3m; BW2 11 samples, depth 5m; GW 11 samples, depth 5m.

are within a factor of ~2 of each other, 0.45-1.15. A value of 0.7±0.3 for $(Ca/Na)_{sol}$ has been used to estimate the Ca contribution to the rivers by silicate weathering. This ratio coupled with Na_s estimated show that silicate Ca in the G-G-I source waters vary widely, 2%-61% of the total Ca in rivers (Fig. 3.13) but on an average accounts for only ~16%. Thus, on an average bulk of the Ca in these waters has to be from sources other than silicates, such as weathering of carbonates and evaporites.

The major sources of Mg to the river waters are weathering of carbonates and silicates. The primary silicate minerals which supply Mg to river water are biotite, chlorite and amphiboles. The silicate Mg in rivers can be estimated following the approaches outlined for Ca. The Mg/Na abundance ratio (Table 3.7) in the three groups of silicate lithologies are indistinguishable from each other within errors, though the value for the HH granites/gneisses appear lower. The Mg/Na ratio in these silicates centre around a value of 0.5±0.3. This compares with the ratio of ~0.6 for the Mg/Na_s in the Jola

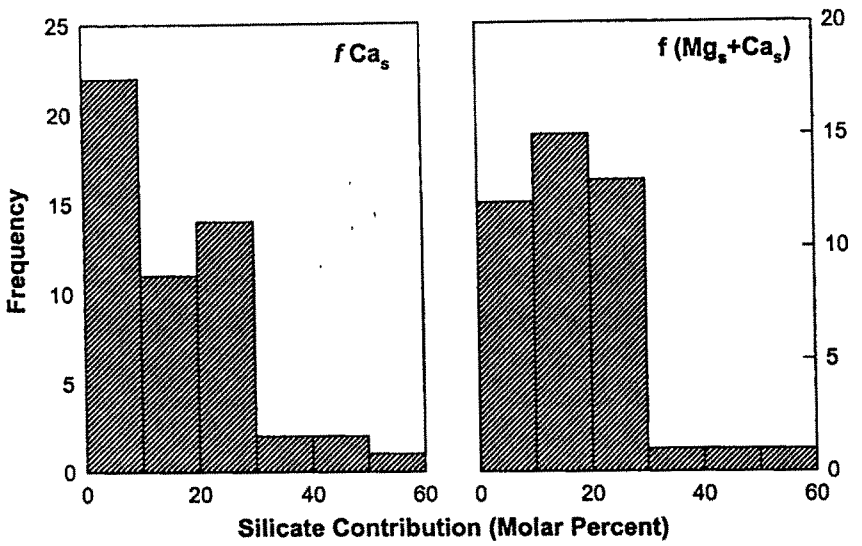

Fig. 3.13: Silicate Ca and Ca+Mg in the headwaters of G-G-I source waters. On an average ~ 16% of Ca and ~17% of (Ca+Mg) in these source waters are of silicate origin.

gad water, which as mentioned earlier, flow predominantly through silicate terrains. The above Mg/Na ratios are much higher than the $(Mg/Na)_{sol}$ derived from the soil profile data (Table 3.8). The Mg/Al in the bed rock and soil profiles are quite similar indicating that loss of Mg during weathering is small and that Mg and Na are not weathered congruently from silicates. The $(Mg/Na)_{sol}$ calculated from data in Table 3.8 range between 0.05-0.17 for the three soil profiles. Based on above three estimates a value of 0.3±0.2 for $(Mg/Na)_{sol}$ is adopted for calculating the silicate Mg component of the G-G-I source waters. The silicate Mg ranges between 2% to 52% of the total Mg with an average of 21%. Analogous to Ca, bulk of Mg in these waters is also derived from sources other than silicates, such as carbonates.

The (Ca+Mg)/Na ratio released to the source waters of the G-G-I from silicates of the Higher and Lesser Himalaya is 1.0±0.35 based on the $(Ca/Na)_{sol}$ (0.7±0.3) and $(Mg/Na)_{sol}$ (0.3±0.2) estimated earlier. This value is used for deriving the silicate contributions of Ca and Mg in rivers draining both the Higher and Lesser Himalaya. With the available data, it is difficult to estimate (Ca+Mg)/Na solution ratios separately for the Higher and Lesser Himalaya; though it is recognized that they may differ because of differences in the composition of bed rocks and intensity of weathering. The (Ca+Mg) derived from silicates vary between 2%-57% of their abundance with an average of 17%

(Fig. 3.13). This, as mentioned earlier, requires that on an average these rivers acquire bulk of their (Ca+Mg) from sources other than silicates, such as carbonates and evaporites. The (Ca+Mg)/Na ratio estimated in this study is similar to that reported (Harris *et al.*, 1998) for the Bhote Kosi river, 0.81±0.2.

(ii) Silicate weathering: Contribution of cations to headwaters

The silicate weathering contribution of cations $(\Sigma Cat)_s$ is calculated as:

$$(\Sigma Cat)_s\,(\mu M/\mu M) = \left[\frac{\Sigma(X_i)_s}{(\Sigma Cations)_r}\right]\times 100 = \left[\frac{(Na_r - Cl_r)\times 2 + 0.85K_r}{(Na_r + K_r + Mg_r + Ca_r)}\right]\times 100$$

The $(\Sigma Cat)_s$ to the G-G-I source waters range between 8% to 67% (Table 3.9, Fig. 3.14) and suggest that on an average about 30% of the cations in these source waters is of silicate origin. This is nearly identical to the $(\Sigma Cat)_s$ in the Ganga waters (30%) at the foot-hills of the Himalaya, sampled at Rishikesh (Fig. 3.1) which integrates the contributions from all its source waters weathering the Higher and Lesser Himalaya. It is also interesting to note that the average silicate component calculated in this study is consistent with the estimates made by Sarin *et al.* (1992). A *lower limit* for the silicate contribution to these waters, as mentioned earlier, is 6%-36% (average 18%) by assuming that *only* Na and K are released to rivers during the weathering of silicates. The main ambiguity in the $(\Sigma Cat)_s$ estimate is that associated with the values of $[(Ca+Mg)/Na]_{sol}$. Propagation of an $+1\sigma$ uncertainty on this value (i.e. $[(Ca+Mg)/Na]_{sol}$ =1.35) would increase the average $(\Sigma Cat)_s$ to 35%, whereas using a value of 0.65 for $[(Ca+Mg)/Na]_{sol}$ (i.e. -1σ uncertainty) decreases the average $(\Sigma Cat)_s$ to 26%. Further, though $(\Sigma Cat)_s$ has been calculated for all the rivers and streams (Tables 3.5 and 3.9), it should be more reliable for the larger rivers which integrate contributions from tributaries draining through different bed rock lithologies.

The $(\Sigma Cat)_s$ in the Bhagirathi along its course centres around 40% for samples collected during the same period, except at Gangotri near its source in the Higher Himalaya where it is marginally higher, ~52% (Table 3.9). The Bhilangna waters derive about 40% of their cations from silicate weathering. The $(\Sigma Cat)_s$ in the Alaknanda sampled at Badrinath in the Higher Himalaya is ~36% which, as in the Bhagirathi,

Table 3.9: Silicate weathering contribution of cations to G-G-I source waters.

Code	River	$(\Sigma Cations)_r$ (μM)	$f(Na_s+K_s)^+$	$f(Ca+Mg)_s^+$	$(\Sigma Cat)_s$	
Ganga					(1)	(2)
13	Bhagirathi	599	89	33	31	52
16	Bhagirathi	740	82	19	20	34
10	Bhagirathi	699	82	23	23	40
11	Bhagirathi	736	74	28	24	43
8	Bhagirathi	709	78	23	22	38
4	Bhagirathi	761	76	22	22	38
5	Bhagirathi	718	78	23	22	39
23	Bhagirathi	724	77	22	22	38
RW-3	Bhagirathi	438	69	12	16	25
14	Kedarganga	647	90	20	25	39
15	Son gad	530	85	11	19	27
17	Helgu gad	246	83	25	27	44
9	Pilang gad	333	84	25	26	43
12	Asiganga	382	82	11	20	29
7	Nagun gad	1023	88	29	24	45
6	Seansu gad	855	82	45	31	59
19	Bhilangna	477	85	22	24	40
22	Bhilangna	521	84	24	25	42
3	Bhilangna	562	83	23	23	40
20	Jola gad	457	77	57	36	67
21	Nailchami gad	768	66	13	17	27
18	Balganga	573	79	22	21	38
28	Alaknanda	261	88	20	21	36
29	Alaknanda	717	83	9	13	21
24	Alaknanda	762	82	14	17	28
RW-4	Alaknanda	656	57	3	7	10
RW-5	Alaknanda	664	53	2	6	8
RW-6	Alaknanda	893	79	5	9	13
RW-7	Alaknanda	276	81	16	18	31
RW-8	Pindar	757	74	5	8	12
2	Ganga	932	82	16	17	30
RW-1	Ganga	585	73	9	13	21
RW-2	Ganga	517	78	11	15	24
1	Song	1585	87	19	17	33
Ghaghara						
RW-9	Sarju	1263	72	4	6	9
RW-10	Ramganga	701	77	19	18	32
RW-11	Kali	1039	83	5	7	11
Indus						
IND-1	Sutlej	981	78	7	13	19

IND-2	Beas	260	55	10	16	23
IND-20	Beas	115	55	10	17	24
IND-3	Chandra	474	64	3	6	8
IND-4	Bhaga	493	71	4	7	10
IND-5	Darcha	287	77	7	12	18

$(\Sigma Cations)_r$ = $(Na_r+K_r+Mg_r+Ca_r)$; *f* and Σ are molar fractions.

$$^{*}f(Na_s+K_s) = \left[\frac{(Na_r - Cl_r)+0.85K_r}{(Na_r+K_r)}\right]\times 100;\ f(Ca_s+Mg_s) = \left[\frac{Na_r - Cl_r}{Ca_r+Mg_r}\right]\times 100$$

$$(\Sigma Cat)_s{}^{*}(1) = \left[\frac{Na_s+K_s}{(\Sigma Cations)_r}\right]\times 100;\ (\Sigma Cat)_s\ (2) = \left[\frac{(Na_r - Cl_r)\times 2+0.85K_r}{(\Sigma Cations)_r}\right]\times 100$$

* minimum silicate contribution assuming only Na and K are released during silicate weathering (i.e. no contribution of Ca and Mg from silicates).

decreases as it traverses through the Lesser Himalaya where it encounters more carbonates in the drainage basin. In general, the $(\Sigma Cat)_s$ in the Alaknanda is less than that in the Bhagirathi and the Bhilangna, consistent with the lithology of its drainage basin which has more carbonates than those in the Bhagirathi and in the Bhilangna basins. The $(\Sigma Cat)_s$ in the Alaknanda show considerable variation, 8% to 36%, the lower values associated with samples collected during the monsoon (September). The silicate cations in the Pindar, a major tributary of the Alaknanda is ~12% (Table 3.9) quite similar to the value for the Alaknanda collected from nearby location during the same season. Among the source waters of the Ghaghara, the Kali and the Sarju have ~10% of their cations from silicates whereas in the Ramganga the $(\Sigma Cat)_s$ is ~32% (Table 3.9). The Indus source waters have $(\Sigma Cat)_s$ 8%-24%, the Chandra sample collected after passing through outcrops of Paleozoic carbonates in the Spiti valley (Kanwar and Ahluwalia, 1979) has the lowest $(\Sigma Cat)_s$ of all the rivers analysed in this study. These results show that there is an overall consistency between the $(\Sigma Cat)_s$ in the rivers and their lithology of the drainage basins.

The $(\Sigma Cat)_s$ in the Bhagirathi, Alaknanda and the Ganga, seems to show seasonal variations (Table 3.10) with lower values in samples collected during the monsoon (September). This observation, if confirmed through more measurements, would suggest

that during stages of high water discharge silicate weathering is relatively less intense probably because of the dominance of physical erosion which may aid in preferentially dissolving the easily weatherable carbonates relative to the more resistant silicates.

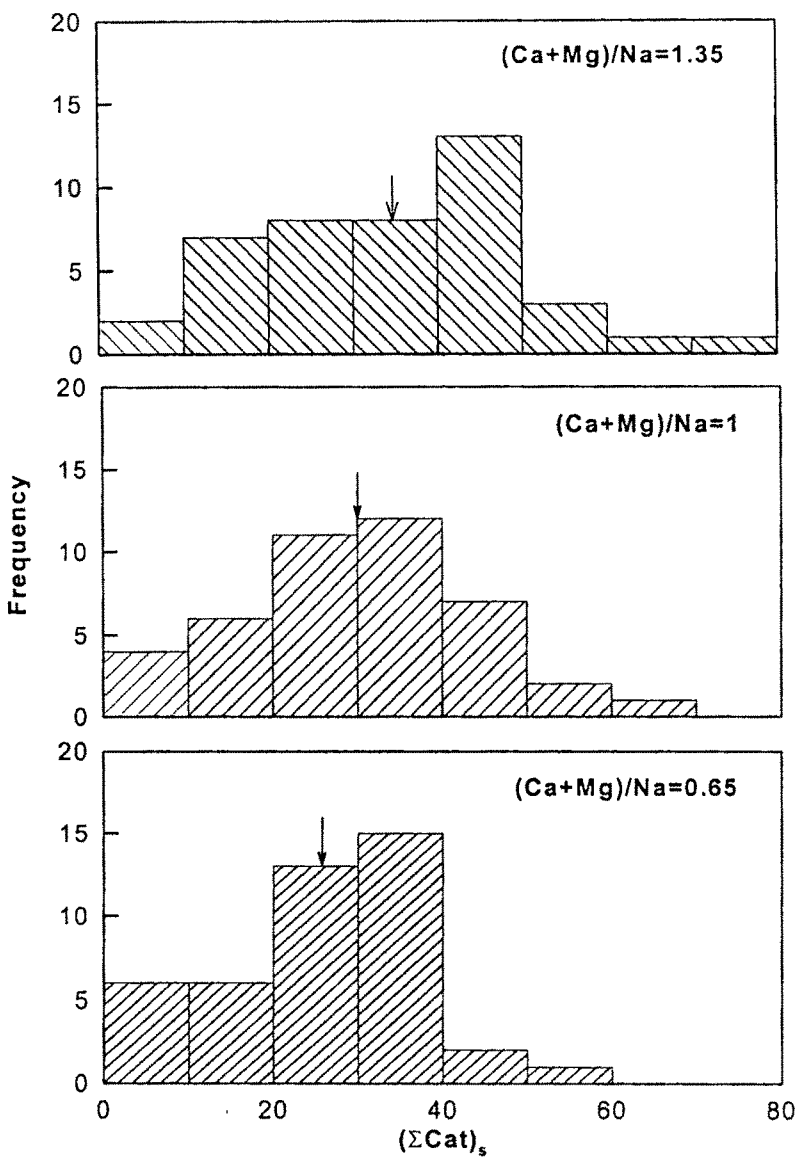

Fig. 3.14: $(\Sigma Cat)_s$ in the headwaters of G-G-I system. The three histograms correspond to estimates based on three values for $(Ca_s+Mg_s)/Na_s$, 0.65, 1 and 1.35. The values 0.65 and 1.35 are $\pm 1\sigma$ uncertainty in the estimates of $(Ca_s+Mg_s)/Na_s$. On an average, $(\Sigma Cat)_s$ accounts for ~30% of the total cations in the source waters (middle figure). The arrows represent the mean of the distribution.

Table 3.10: Seasonal variation in $(\Sigma Cat)_s$ in the Ganga source waters

River (Location)	Sampling date	% $(\Sigma Cat)_s$	Ref.
Bhagirathi (Devprayag)	March, 82	36	Sarin *et al.*, 1989
	Nov, 83	37	Sarin *et al.*, 1989
	April, 89	38	Sarin *et al.*, 1992
	Sept, 96	25	this study
Alaknanda (Bhagwan)*	Nov, 83	27	Sarin *et al.*, 1989
	April, 89	28	Sarin *et al.*, 1992
Alaknanda (Devprayag)*	Sept, 96	10	this study
Ganga (Rishikesh)	March, 82	29	Sarin *et al.*, 1989
	Sept, 82	17	Sarin *et al.*, 1989
	Nov, 83	28	Sarin *et al.*, 1989
	April, 89	30	Sarin *et al.*, 1992
	Sept, 96	21	this study

* Devprayag is about ~10 km downstream of Bhagwan.

In the preceding paragraphs the $(\Sigma Cat)_s$ in the source waters of G-G-I have been constrained using better controls on the (Ca/Na) and (Mg/Na) ratios released to the rivers during silicate weathering. These results suggest that on an average about a third of the cations in these rivers is of silicate origin and bring to focus the significance of silicate weathering in these basins in contributing to the cation budget of these rivers. The $(\Sigma Cat)_s$ values obtained depend critically on the values of $(Ca/Na)_{sol}$ and $(Mg/Na)_{sol}$. As mentioned earlier, a single value is used for these ratios for all the source waters draining through both the Higher and Lesser Himalaya. Such an assumption, though may be an oversimplification, it places useful constraints on the cation contributions via silicate weathering to these source waters. Further, the uncertainty of ±35% in the $[(Ca+Mg)/Na]_{sol}$ is likely to account for the variations in the Ca and Mg inputs from the different lithologies.

(iii) Carbonate (Ca+Mg) in the headwaters

Carbonates occur widespread in the Lesser Himalaya and is a dominant lithology in the drainage basins of the several headwaters of the G-G-I system. These carbonates are predominantly dolomites and can contribute both Ca and Mg to the rivers which flow

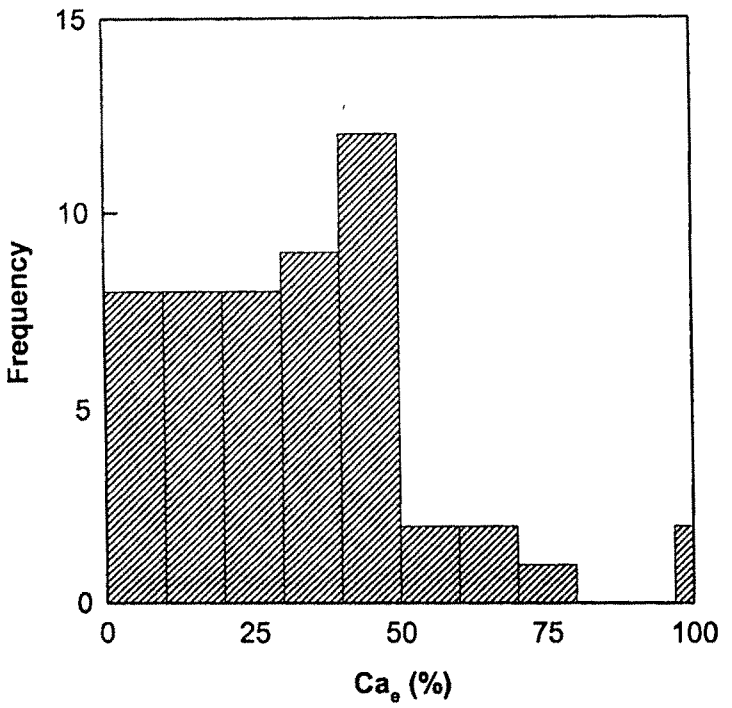

Fig 3.15: Frequency distribution of molar fraction of evaporite Ca in the source waters. These calculations assume that all the SO_4 in the water is from the dissolution of evaporites and hence are upper limits.

through them. The carbonate component of Ca to the rivers is difficult to estimate as both carbonates and evaporites (in addition to silicates discussed above) can contribute to its mass balance in rivers, whereas for Mg, carbonates are the only other source. Many of the G-G-I source waters have high SO_4 concentration, 18 to 460 μM (Sarin *et al.*, 1992), and account for 1% to 67% (molar fraction) of the anion budget of these rivers. The SO_4 in these waters can originate from (i) dissolution of evaporites, in this case equimolar concentration of Ca and SO_4 would be released to the waters, (ii) oxidation of sulphide minerals in the basin and (iii) from sulphurous springs. The observation (Sarin *et al.*, 1992) that in two samples, Bhagirathi and Kedarganga, collected at Gangotri after they flow through the Higher Himalaya, SO_4 concentration exceeds Ca (SO_4/Ca = 1.2 - 1.3 μM /μM), suggests that a significant component of SO_4 in these waters has to be from oxidation of sulphide minerals and/or from sulphurous springs. Data on the abundance and distribution of evaporites and sulphide minerals in the drainage basin are sparse, however, presence of pyrites and other sulphide minerals disseminated in shales,

quartzites and other sedimentary rocks of the basins (Tewari and Gaur, 1977) and deposits of gypsum in dolomites of Krol formation have been reported (Valdiya, 1980). An *upper limit* on the evaporite component of Ca in river can be derived by assuming that all the SO_4 in the water is from its dissolution. This upper limit is presented in Fig. 3.15, which shows that in the Bhagirathi, Bhilangna, Alaknanda and a few source waters of the Indus, and the Ghaghara, the gypsum Ca is quite high, averaging about ~34% (molar fraction), comparable to or even more than the carbonate component of Ca [$Ca_c = Ca_r - (Ca_s + Ca_e)$; $Ca_e = SO_4$]. This is unlikely considering that gypsum/anhydrite is expected to be less abundant relative to carbonates in the drainage basins of the rivers, though their occurrence has been reported (Valdiya, 1980) from several locations of the Lesser Himalaya. The observation that waters with high SO_4 (>100 μM) generally have low Cl, with SO_4/Cl 3.5 to 77, and low to moderate TDS (≤100 mg/l) are other indications that evaporites may not be an important source of SO_4 to these waters. Thus, Ca_e in these waters is very likely to be lower than that calculated assuming it to be equivalent to SO_4. This inference, if valid, would suggest that significant fraction of SO_4 in these rivers is from the oxidation of pyrites. Here again, to account for the measured concentration of SO_4 in the waters, the pyrite abundance has to be adequate in the drainage basins. Pyrite disseminated in the shales of the Lesser Himalaya from several locations though are reported, more data on its abundances along the drainage basins are needed to better assess their role in contributing to the SO_4 in these waters. Thus, with the available data it is not possible to calculate separately the input of SO_4 to the rivers via dissolution of evaporites and oxidation of pyrites. Studies on sulphur isotopes in the dissolved sulphate of these rivers may help resolve this issue.

In the present study, therefore only an *upper limit* on the carbonate Ca could be estimated assuming that the rivers receive Ca only two sources, silicates and carbonates (i.e. there is no contribution of Ca to the rivers via dissolution of evaporites). The calculated carbonate Ca ranges between 39% to 98% of Ca_r. In rivers where SO_4 concentrations are relatively low compared to Ca, the upper limit on Ca_c estimated above would be close to the true carbonate component of Ca in them. The $(Ca+Mg)_c$ in the source waters (upper limit) range between 71 to 1123 μM. This accounts for 43% to 98% (molar fraction) (Ca+Mg) in the rivers.

(iv) Sr and $^{87}Sr/^{86}Sr$ of the Ganga, Ghaghara and the Indus source waters

In this section, the impact of silicate and carbonate weathering on the Sr budget of the G-G-I river system is assessed. The silicate and carbonate Sr have been calculated based on the approach followed for major ions. Endmember values are assigned based on the three approaches, i.e. their values in granite/gneisses of the Higher and Lesser Himalaya, water composition flowing through mainly silicate lithology and from the soil and its parent rock chemistry. It must be mentioned here that in section 3.1 (iii), it was concluded based on Sr/Ca and $^{87}Sr/^{86}Sr$ in Precambrian carbonate outcrops that these carbonates are unlikely to be a dominant source for the high radiogenic Sr isotope composition of the G-G-I headwaters.

Figure 3.16 is a comparison of the frequency distribution of $^{87}Sr/^{86}Sr$ in the source waters of the Bhagirathi, Alaknanda, Ghaghara and the Indus and those in the carbonates and whole rock granites/gneisses from the Lesser and Higher Himalaya. Sr isotopic data of whole rocks from the Lesser and Higher Himalaya have been used for comparison, as a large fraction of the drainage basins of the Bhagirathi, Alaknanda, Ghaghara and Sutlej is in these regions. France-Lanord *et al.* (1993) concluded that the primary source of the sediments to the Bay of Bengal are the higher Himalayan Crystallines (or its close analogue with only minor contributions from the Lesser Himalaya) based on studies of clay mineralogy, Sr, Nd and oxygen isotope systematics in them. More recently, Derry and France-Lanord (1996), while attesting to the earlier conclusions of France-Lanord *et al.* (1993) regarding the provenance of detritus in the Bay of Bengal sediments, alluded to the possibility of a relative increase in the contribution of the Lesser Himalaya materials to the Bay of Bengal sediments during the Pliocene. Many of the G-G-I source waters have significant fraction of the drainage in the Lesser Himalaya. Chemical weathering is likely to more pronounced in the Lesser Himalaya where the general temperature is higher than the Higher Himalaya the difference in temperature could result in increase in dissolution rate (Lasaga *et al.*, 1994). Soil formation in the Lesser Himalaya (Gardner and Walsh, 1996) and availability of more biogenic CO_2 could also enhance the chemical weathering in this part of the Himalaya compared to the Higher Himalaya. It is therefore possible that sites of maximum mechanical erosion and maximum chemical weathering are decoupled, with Lesser Himalaya contributing more to the dissolved load than the

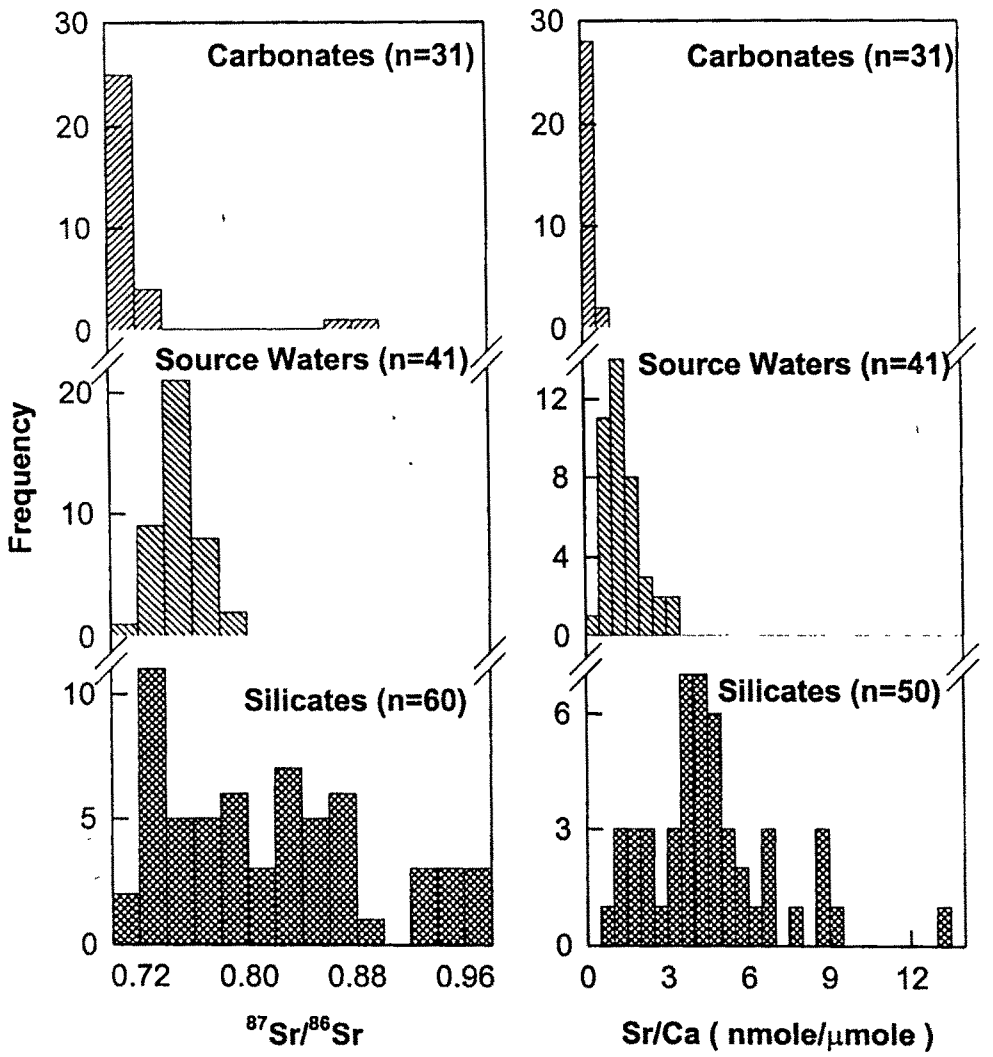

Fig. 3.16: Comparison of $^{87}Sr/^{86}Sr$ and Sr/Ca in G-G-I source waters, silicates (granite/gneisses) and Precambrian carbonate outcrops of the Lesser Himalaya. The data show that bulk of the carbonates have $^{87}Sr/^{86}Sr$ and Sr/Ca much less than those measured in the headwaters whereas those in silicates bracket the source water values. Granites/gneisses having $^{87}Sr/^{86}Sr$ >1.0 though reported, are excluded from the histogram.

Higher Himalaya. The observation, however, that the Bhagirathi (at Gangotri) and Alaknanda (at Badrinath) have high $^{87}Sr/^{86}Sr$ with moderately high Sr concentration before they enter the Lesser Himalayan basin (Krishnaswami *et al.* 1992) points to the important influence the rocks in the Higher Himalaya also have in regulating the Sr isotope composition of these rivers. Currently, however, the relative contributions from the drainage basins of the Higher and Lesser Himalaya to the Sr flux and isotopic

composition of these rivers are uncertain as data on their water flux along the flow path is unavailable.

The Sr isotope composition of the source waters overlaps with those of the granites/gneisses, but are significantly higher than that in most of the carbonates. A similar pattern is also seen in the comparison of the Sr/Ca ratios (Fig. 3.16), the source waters have a mean Sr/Ca ratio (1.41±0.69) nmol/μmol that is much higher than that of the carbonates (0.20±0.15) nmol/μmol.

In order to better constrain the sources of Sr to these rivers similar approach has been followed as for major ions to characterise the silicate end member values. The Sr/Na ratios (mole) in the HH and LH granites and gneisses show considerable range, over two orders of magnitude (Table 3.7). The mean Sr/Na, after discarding the extreme values on either end of its distribution are 1.22±0.65 and 1.68±0.72 respectively for the HH and LH samples (Table 3.7) and overlap with each other within errors. The Sr/Na in the Jola gad waters is 1.96 (Singh *et al.*, 1998). The (Sr/Na) solution ratio based on the results from three soil profiles (Gardner and Walsh, 1996) is in the range of 2.5-2.9. The difference between the three values may be due to the incongruent weathering of the Sr and Na or regional differences in Sr/Na in source rocks. Following the same assumptions used for the major ions, the ratio of (Sr/Na) released to rivers from weathering of silicates can be in the range of 1.2-2.9. For estimating the silicate Sr in the rivers we have adopted a value of 2.0±0.8 This is 25% lower than that used by Singh *et al.* (1998), but falls within ±1σ uncertainty. The Sr_s in the source waters range between 2% to ~100% of Sr_r with a mean of ~40% (Table 3.11). In the Bhagirathi (Devprayag), Bhilangna (Tehri), Alaknanda (Bhagwan) and the Ganga (at Rishikesh) the Sr_s constitutes 43±17%, 71±28%, 27±11% and 34±14% of Sr_r respectively. Among the Ganga source waters, Bhilangna has bulk of its Sr from silicates (~70%), whereas in the Bhagirathi silicate Sr accounts for about half of its Sr budget. In the Alaknanda, the silicate Sr decreases from ~55% in the samples collected at Badrinath, to ~27% at Devprayag, following the trend in $(\Sigma Cat)_s$. The Sr_s contribution to the Sr budget in the Sutlej, Beas, Chandra and Bhaga; the source waters of the Indus are small, ≤20% (Table 3.11), consistent with the estimates for $(\Sigma Cat)_s$ in these waters.

The significance of silicate weathering in determining the $^{87}Sr/^{86}Sr$ of the G-G-I source waters can be gauged from the trend in Fig. 3.17 which shows a strong positive correlation of $^{87}Sr/^{86}Sr$ with $(\Sigma Cat)_s$ ($r = 0.75$). It is borne out from this trend that silicate weathering is primarily responsible for the high $^{87}Sr/^{86}Sr$ in the source waters (a plot of $^{87}Sr/^{86}Sr$ vs. Sr_s also shows similar trend). It is noteworthy that the end member values of $^{87}Sr/^{86}Sr$ for $(\Sigma Cat)_s = 0$ and $(\Sigma Cat)_s = 100\%$ derived from Fig. 3.17 are 0.715 and 0.82 respectively, close to the mean ratios in the Precambrian carbonates and granites/gneisses in the Lesser Himalaya (Krishnaswami and Singh, 1998).

Importance of carbonates in regulating the Sr budget of the rivers can be evaluated by estimating the carbonate Sr in them. The primary sources of Sr to rivers are silicates, carbonates and evaporites. As discussed earlier, it is not possible to estimate the evaporite contribution to major ions (and Sr) from the available data. Carbonate Sr can be calculated based on the carbonate Ca component of rivers which equals the difference between the measured Ca in them and their calculated silicate Ca. The Sr input to these rivers from carbonates is calculated as:

$$Sr_c(nM) = (Ca_r - Ca_s) \times \left(\frac{Sr}{Ca}\right)_c$$

$$= [Ca_r - (0.7 \pm 0.3)Na_s] \times \left(\frac{Sr}{Ca}\right)_c \qquad (12)$$

$(Sr/Ca)_c$ is taken to be the abundance ratio in Precambrian carbonate outcrops, (0.2±0.15) nmole/μmole. It is assumed in this calculation that Ca_r in rivers is derived from two components, Ca_s and Ca_c. The results of these calculations yield value of 5% to 42% (mean 15%) for the carbonate Sr contribution. The contribution of silicate and carbonate Sr in the source waters are compared in Fig. 3.18. The data inspite of substantial uncertainty, show that in most of the source waters the silicate Sr component exceeds that of the carbonate Sr, exceptions being some of the tributaries of the Ghaghara and the Indus, where $Sr_s \approx Sr_c$ (Krishnaswami and Singh, 1998). Thus the extensive outcrops of the Precambrian carbonate deposits of the Lesser Himalaya, as inferred earlier (section 3.1 (iii)) in general is not a major source for both Sr and $^{87}Sr/^{86}Sr$ of the G-G-I source waters.

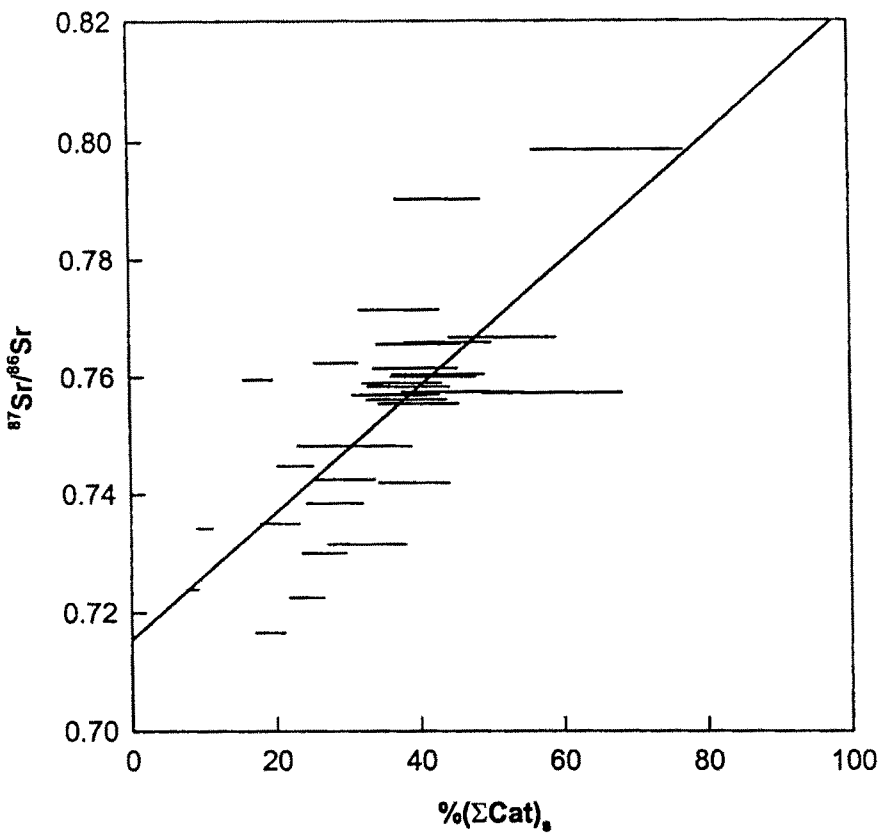

Fig. 3.17: Variation of measured $^{87}Sr/^{86}Sr$ in G-G-I source waters with their calculated $(\Sigma Cat)_s$ [Table 3.9 (2)]. There is an overall positive correlation between the two ($r = 0.75$) suggesting that silicate weathering is an important source for the highly radiogenic $^{87}Sr/^{86}Sr$ of the rivers (Krishnaswami and Singh, 1998). The horizontal bars represent the range in $(\Sigma Cat)_s$ calculated by considering $\pm 1\sigma$ uncertainty.

It is seen from the data in Table 3.11 that for many rivers the (Sr_s+Sr_c) do not add upto 100%, though in some of them Sr balance can be achieved within uncertainties.

The fraction of riverine Sr that is supplied from the weathering of silicates and Precambrian carbonates is presented in Fig. 3.19 which show that only in a few of the source waters the Sr budget can be balanced if input is solely from these sources. It is possible to balance the Sr budget in a few more rivers in which the sum of silicate and carbonate Sr contribution exceed 70% by considering 1σ uncertainties associated with the estimates (Fig. 3.19). It is seen from this exercise that in a number of source waters, particularly Kali, Gori (Ghaghara system), Sutlej, Beas, Chandra, Bhaga and Dharcha (Indus system) it is difficult to account for their measured Sr if the two end members

chosen (silicates and Precambrian carbonates) are their only sources and if the approaches used for estimating their contributions are valid (Krishnaswmi and Singh, 1998 and Krishnaswami *et al.*, 1998). These results seem to suggest that in addition to silicates and the Precambrian carbonates, some of the rivers may be receiving Sr supply from sources such as evaporites, phosphates and carbonates (other than the Precambrian outcrops) and the assumption of a two component system for Ca and Sr may not be valid.

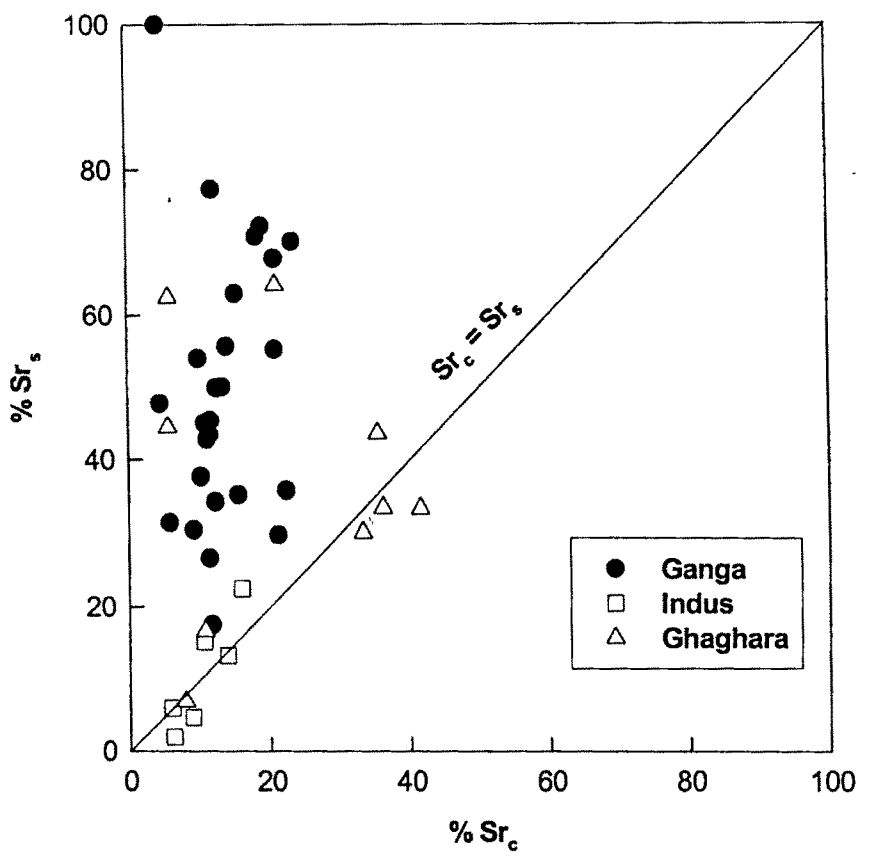

Fig. 3.18: Scatter plot of Sr_s vs Sr_c. The silicate Sr exceed the carbonate Sr in a majority of the headwaters. The data for the Ganga, Ghaghara and the Indus headwaters are shown by by separate symbols. In the Kali, Gori (Ghaghara system) Sutlej, Beas, Chandra, Bhaga, Dharcha (Indus system) $Sr_s \approx Sr_c$.

This, as discussed below, is also evident from the Sr isotope data. In Fig. 3.20 $^{87}Sr/^{86}Sr$ of the G-G-I source waters is plotted as a function of their measured Ca/Sr ratios (Krishnaswmi and Singh, 1998 and Krishnaswami *et al.*, 1998). Also presented in the Fig. 3.20 are the Sr isotope and Ca/Sr values for silicate (granites and gneisses from HH and LH) and Precambrian carbonate end members. The silicate endmember has Ca/Sr

centring around 0.25 (μM/nM) with $^{87}Sr/^{86}Sr$ close to 0.80 based on data for about 50 granites/gneisses each from the LH and the HH. The river water data do not fall on the mixing line between the silicate and Pc-Carbonate end members (Fig. 3.20), but seem to be contained in a triangle bound by silicate, carbonate and an additional end member. The $^{87}Sr/^{86}Sr$ and Ca/Sr of the additional end member as seen from Fig. 3.20 is ~0.715 and ~0.2 (μmole/nmole) respectively. The low $^{87}Sr/^{86}Sr$ and Ca/Sr (i.e.high Sr) end member

Table 3.11: Silicate and carbonate weathering contribution of Sr to G-G-I source waters

River	Sr_r* (μM)	$f Sr_s$	$f Sr_c$	$f(Sr_s+Sr_c)$
Bhagirathi	331	77	12	90
Bhagirathi	694	31	9	40
Bhagirathi	524	45	11	56
Bhagirathi	503	54	10	64
Bhagirathi	502	45	12	57
Bhagirathi	560	43	11	54
Bhagirathi	420	56	14	70
Bhagirathi	529	44	12	55
Kedarganga	262	70	24	94
Son gad	315	30	21	51
Helgu gad	168	50	13	63
Pilang gad	181	63	15	78
Asiganga	184	36	22	58
Nagun gad	1390	32	6	38
Seansu gad	1000	48	5	52
Bhilangna	224	68	21	89
Bhilangna	246	72	19	92
Bhilangna	265	71	18	89
Jola gad	273	102	5	106
Nailchami gad	431	35	16	51
Balganga	367	50	13	64
Alaknanda	141	55	21	76
Alaknanda	650	18	12	29
Alaknanda	644	27	12	38
Ganga	676	34	12	47
Song	1310	38	10	48
Sarju	263	34	42	75
Ramganga	296	64	21	85
Ghat gad	316	44	36	79
Kali	1320	7	8	15
Gori	768	17	11	27
Sarju	311	30	33	64

Sarju	286	34	36	70
Panar	1245	45	6	50
Suyal	413	63	6	68
Sutlej	1962	6	6	12
Beas	169	23	16	38
Chandra	1118	2	6	8
Bhaga	718	5	9	14
Dharcha	255	13	14	27
Beas	105	15	11	26

* Krishnaswami *et al.* (1992); Pande *et al.* (1994) and Trivedi *et al.* (1995)
$f Sr_s = (Sr_s/Sr_r) \times 100$
$f Sr_c = (Sr_c/Sr_r) \times 100$
$f (Sr_s+Sr_c) = [(Sr_s+Sr_c)/Sr_r] \times 100$

is commonly taken to be carbonates. The results of this study (Fig. 3.20) suggest that the extensive outcrops of Precambrian carbonates of the Lesser Himalaya because of their relatively lower Sr abundance (i.e. high Ca/Sr) is not this additional end member. Possible candidates for this endmember are Tethyan/Tibetan carbonates (present in the drainage basins of some of the Ghaghara and Indus source waters) and/or evaporites rich in Sr (gypsum, celestite). Harris *et al.* (1998) reported a range of values for $^{87}Sr/^{86}Sr$ in Tibetan carbonates based on measurements of acid leaches of bedload samples of the Bote Kosi river in the Tibetan Sedimentary Series. The studies of Galy (1999), indeed, show that the Tibetan carbonates have Sr concentrations ranging from 252 to 1600 ppm with $^{87}Sr/^{86}Sr$ varying from 0.7079-0.715 which can satisfy the values required for the third endmember. Very recently, Blum *et al.* (1998) based on the chemical and Sr isotope study of Raikhot watershed from the Higher Himalayan Crystallines have suggested that weathering of vein calcites contributes to their high $^{87}Sr/^{86}Sr$. The Raikhot waters have Ca/Sr (1.4-3.6 μM/nM) slightly higher than that in the Ganga headwaters (0.32-2.2 μM/nM). Further, the drainage basin of the Raikhot river is only in the Higher Himalaya, whereas the G-G-I headwaters discussed in this study flow through both the Higher and Lesser Himalaya with large fraction of their drainage in the Lesser Himalaya. Blum *et al.* (1998) also conducted leaching experiments on gneisses and granites and bed load samples and came to the conclusion that these samples have a highly radiogenic leachable Sr component, which they attributed to vein calcites. Based on the $^{87}Sr/^{86}Sr$ and Ca/Sr of the Raikhot river waters the authors (Blum *et al.*, 1998) suggested that vein

calcites with $^{87}Sr/^{86}Sr$ (~0.8) and Ca/Sr ~5 would be an endmember to explain the Raikhot river data. The vein calcite is a high $^{87}Sr/^{86}Sr$, low Sr endmember (Ca/Sr ~5 μmol/nmol), properties which are quite opposite to that required for the endmember in Fig. 3.20, low $^{87}Sr/^{86}Sr$ and high Sr (i.e. low Ca/Sr). These results suggest the need to get more data on the distribution and Sr isotope systematics of the vein calcites directly and

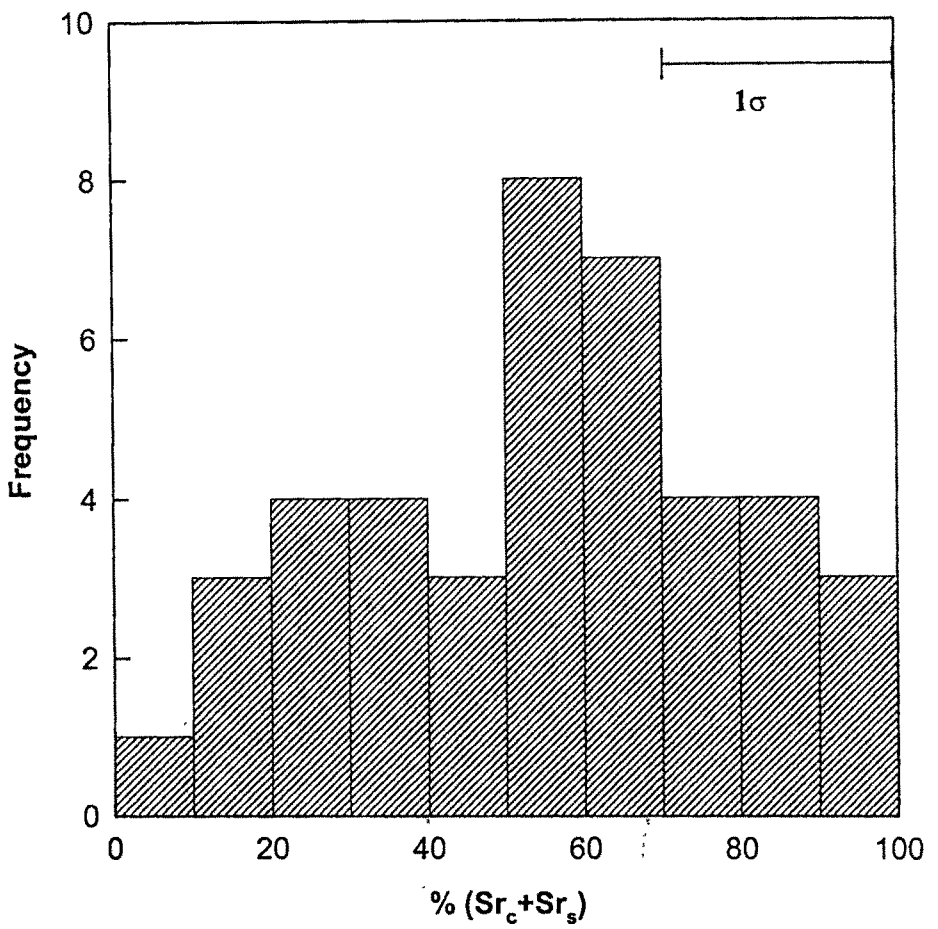

Fig. 3.19: The sum of silicate and carbonate Sr contribution to the Sr budget of the G-G-I source waters. The data show that only in very few of the headwaters, thr Sr budget can be balanced based on the approaches discussed in the text. Samples with (Sr_s+Sr_c) contribution >70% can be made to balance the budget by considering 1σ uncertainty.

also look for differences if any in the Sr isotope contribution from various sources to the rivers of the Higher and the Lesser Himalaya.

The inferences about the need for a third source based on Fig. 3.20 rests on the assumption that the silicate and carbonate end members have unique $^{87}Sr/^{86}Sr$ and Ca/Sr

values. If this assumption is not valid, for example, if the silicates can have $^{87}Sr/^{86}Sr$ ranging between 0.75-0.80 with Ca/Sr 0.2-2.0, the observed trend (Fig. 3.20) can result from mixing of these silicates with an end member having $^{87}Sr/^{86}Sr$ of ~0.715 with Ca/Sr ~0.2. This suggestion, as in the previous case, also requires an end member with low $^{87}Sr/^{86}Sr$ and low Ca/Sr. An alternative hypothesis is to suggest that the Sr isotope

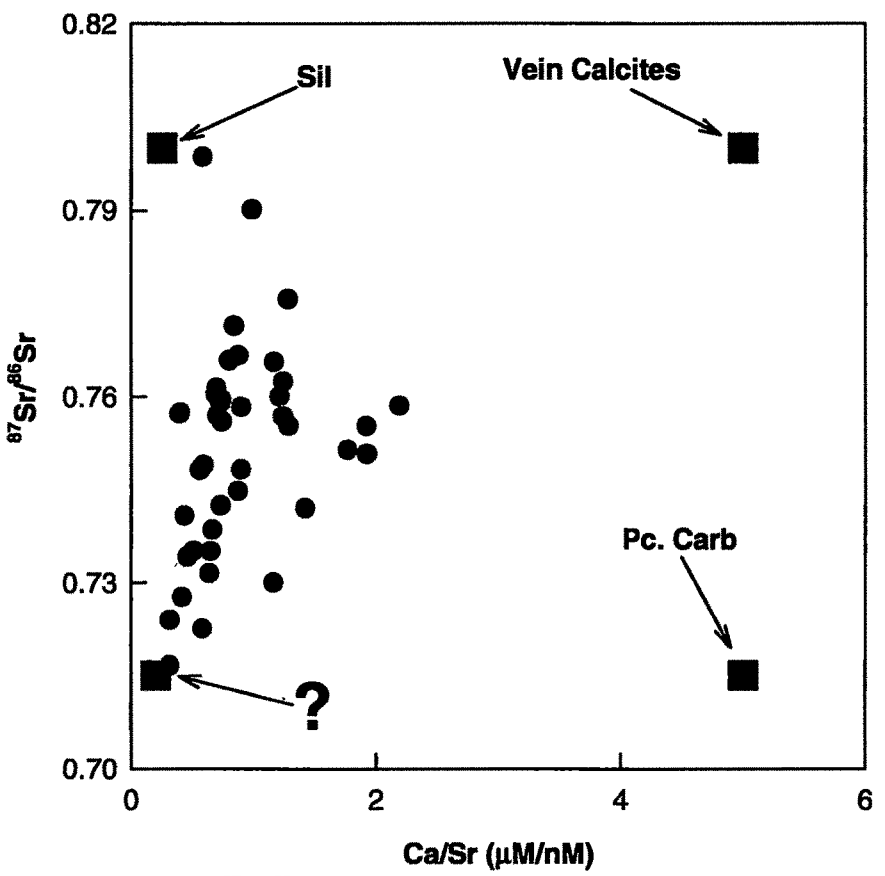

Fig. 3.20: Plot of reported $^{87}Sr/^{86}Sr$ vs Ca/Sr in the G-G-I headwaters. The endmember values for silicates (Sil), Precambrian Carbonates (Pc. Carb.) and vein calcites (Blum *et al.*, 1998) are also given. The river water data do not plot on the mixing line of silicate and Precambrian carbonates, but fall in the field of a triangle defined by silicate, Precambrian carbonate and an additional third endmember. Possible candidates for this endmember are Tethyan/Tibetan carbonates and/or Sr rich evaporite phases.

composition of the headwaters result from mixing of silicates (Ca/Sr = 0.25, $^{87}Sr/^{86}Sr$=0.80±0.02), vein calcites (Ca/Sr=5, $^{87}Sr/^{86}Sr$=0.80) and a third endmember (Ca/Sr ≅ 0.2, $^{87}Sr/^{86}Sr$ ≅ 0.715). Both the above suggestions discount the significance of contribution of Ca and Sr to rivers from the weathering of Precambrian carbonates of the Lesser Himalaya, which is unlikely to be realistic for the G-G-I source waters which have

a significant fraction of their drainage through Precambrian carbonates. Further, the available data show that silicates from the LH and HH rarely have Ca/Sr > 0.8 (μmole/nmole; Fig 3.16).

It is borne out from the above discussions and material balance calculations that silicate weathering contributes more to the present day Sr budget of many of the G-G-I source waters than weathering of Precambrian carbonate outcrops and that it plays an important role in determining their $^{87}Sr/^{86}Sr$. The variations in the Sr concentration and $^{87}Sr/^{86}Sr$ of these source waters seem to be dictated by three end members, silicate (Ca/Sr = 0.25, $^{87}Sr/^{86}Sr$=0.80±0.02), Precambrian carbonates (Ca/Sr = 5, $^{87}Sr/^{86}Sr$ = 0.715±0.01) and a third component (Ca/Sr ≅ 0.2, $^{87}Sr/^{86}Sr$ ≅ 0.715).

In this section attempts to establish a mass balance for Sr in the headwaters of the Ganga-Ghaghara-Indus system, based on contributions from silicates and carbonates, is presented. As evident, this is a difficult exercise as Ca and Sr in these waters have multiple sources with their own characteristic $^{87}Sr/^{86}Sr$. Our data and calculations show that silicate weathering exerts a more dominant control relative to carbonate weathering on the present day Sr-mass balance and their $^{87}Sr/^{86}Sr$ (Table 3.11) in the source waters of the Ganga, whereas in Kali & Sarju (of Ghaghara) and Sutlej (of Indus) the contributions from silicate and carbonate weathering to their Sr budget seem comparable.

3.3. SILICATE AND CARBONATE CHEMICAL WEATHERING RATES IN THE GANGA SOURCE WATER BASINS

The present day chemical weathering rates of silicates and carbonates in river basins can be determined from the silicate and carbonate components of their major cations, silica concentration and data on their water fluxes and drainage areas. Among the source waters discussed in this study water flux data is available only for the Bhagirathi and the Alaknanda at Devprayag (Sarin *et al.*, 1992). The discharge of the Ganga at Rishikesh, a few tens of kilometers downstream of Devprayag is taken to be same as the sum of the discharges of the Bhagirathi and the Alaknanda which merge together at Devprayag to form the Ganga. The silicate weathering rates (SWR) are calculated by summing the Na, K, Mg and Ca contributions from silicate weathering and silica concentration (in units of mg/l); the carbonate weathering rates (CWR), from the carbonate Ca and Mg contributions and stoichiometric equivalent of carbonate. (The

carbonate Ca and Mg are obtained by subtracting the silicate Ca and Mg from their measured concentrations in the rivers. As mentioned earlier, the carbonate Ca calculated this way would be an upper limit if Ca is also supplied to the waters via evaporite dissolution). The results show that in the Bhagirathi and the Alaknanda basins silicate weathering contributes to 35 and 26 wt% of cations (corresponding to 31% and 22% of cation charge). These, coupled with silica concentrations, yield values of 4-6 mm/ky for SWR in these river basins (Table 3.12); 3-6 times lower than the carbonate weathering rates (Krishnaswami *et al.*, 1998).

Table 3.12: Silicate and carbonate weathering rates*

River	Discharge (10^{12} l/y)	Area (10^3 km^2)	SWR		CWR	
			(a)	(b)	(a)	(b)
Bhagirathi$^+$	8.3	7.8	15.2	5.8	41.1	15.2
Alaknanda$^+$	14.1	11.8	10.2	3.9	63.2	23.4
Ganga$^+$	22.4	19.6	12.9	4.9	51.7	19.1
G-B^{++}	1002	1555	13.6	5.3	31.7	11.7

* mean density for silicates and carbonates 2.6 and 2.7 gm cm^{-3} respectively; (a) tons/km^2/y; (b) mm/ky.
$^+$ calculated based on composition at Devprayag, Bhagwan and Rishikesh respectively.
$^{++}$ calculated for the entire basin based on composition at Patna and Goalpara (Sarin *et al.*, 1989).

The drainage basins of these rivers, thus, are getting chemically weathered at a rate of ~25 mm/ky. (These weathering rate calculations are based on limited data both for discharge and the chemical composition of the rivers. More seasonally representative data for all these parameters, particularly the major ion chemistry of the rivers during their peak discharge, are required to obtain a better time averaged estimate of the weathering rates). Sarin et al (1992) had reported chemical denudation rates of ~50 mm/ky for these

river basins, a factor of ~2 higher than that calculated in this study. The difference between the two estimates is because the calculations of Sarin et al (1992) are based on the flux of total dissolved solids which include, in addition to cations, silica and carbonate from the chemical weathering of silicates and carbonates; contributions from the atmosphere (cyclic salts), alkalinity associated with silicate and carbonate weathering evaporite dissolution and/or pyrite oxidation. The contemporary silicate weathering rates of the Bhagirathi and the Alaknanda basins are comparable to those reported for other major world river basins, 1-7 mm/ky in the Guayana Shield (Edmond *et al.*, 1995) and 0.2-8 mm/ky in the Amazon basins (Gailardet *et al.*, 1997), and 1.3-2.4 mm/ky in the Congo (Gaillardet *et al.*, 1995). The CO_2 consumption rates for silicate weathering in the Bhagirathi and the Alaknanda basins (calculated assuming that silicates are weathered only by CO_2) are 4.1×10^5 and 3.6×10^5 mole/km^2/y. If this calculation is extended to the entire Ganga-Brahmaputra basin, the proportion of cations supplied via silicate weathering is estimated to be 37 wt% (34% of cation charge) and the corresponding CO_2 consumption rates by silicate weathering would be 3.3×10^5 moles/km^2/y (using average composition of these waters at Patna and Goalpara, ref. Sarin *et al.*, 1989). These estimates are likely to be on the higher side as (i) part of silicate weathering could be brought about by sulphuric acid from oxidation of pyrites and (ii) the assumption that chloride corrected Na is entirely of silicate origin may not be valid for the Ganga basin, which is known to have alkaline/saline soils in the plains (Sarin *et al.*, 1989). Edmond and Huh (1997) estimated a CO_2 consumption rate of $(1\text{-}3)\times10^5$ moles/km^2/y due to silicate weathering for the Himalayan collision zone.

It is apparent from the above preliminary calculations that the present day CO_2 consumption by silicate weathering in the G-B basin is of the same order as those in other major river basins, 0.2×10^5 to 2.3×10^5; 0.02×10^5 to 0.8×10^5; 0.1×10^5 to 2.1×10^5 moles/km^2/y in the Amazon (Gaillardet *et al.*, 1997), Congo (Gailardet *et al.*, 1995) and the Guyana (Edmond *et al.*, 1995) basins respectively. More precise estimates of CO_2 consumption rates in the G-B basin need better constraints on the proportions of silicate weathering by CO_2 and sulphuric acid and on the supply of various cations from silicates from the Higher and Lesser Himalaya and the plains.